CHALMERS
UNIVERSITY OF TECHNOLOGY

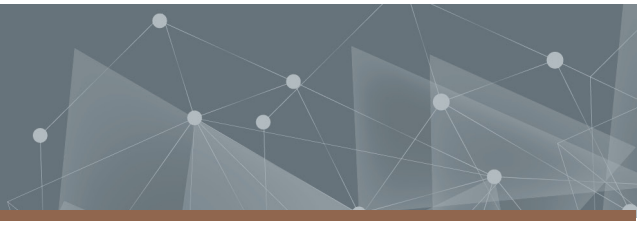

Optimal Thermal Management and Charging for Battery Electric Vehicles

Master's thesis in Systems, Control and Mechatronics

Victor Hanson
Jiaming Zhao

DEPARTMENT OF ELECTRICAL ENGINEERING

CHALMERS UNIVERSITY OF TECHNOLOGY
Gothenburg, Sweden 2022
www.chalmers.se

Master's thesis 2022

Optimal Thermal Management and Charging for Battery Electric Vehicles

Victor Hanson
Jiaming Zhao

CHALMERS
UNIVERSITY OF TECHNOLOGY

Department of Electrical Engineering
Chalmers University of Technology
Gothenburg, Sweden 2022

Optimal Thermal Management and Charging for Battery Electric Vehicles
Victor Hanson
Jiaming Zhao

Supervisors: Jimmy Forsman, Volvo Cars
Ahad Hamednia, Electrical Engineering
Examiner: Nikolce Murgovski, Electrical Engineering

Master's Thesis 2022
Department of Electrical Engineering
Chalmers University of Technology
SE-412 96 Gothenburg
Telephone +46 31 772 1000

Typeset in LaTeX
Printed by Chalmers Reproservice
Gothenburg, Sweden 2022

Optimal Thermal Management and Charging for Battery Electric Vehicles
Victor Hanson
Jiaming Zhao
Department of Electrical Engineering
Chalmers University of Technology

Abstract

This thesis proposes a solution for thermal management and charging in battery electric vehicles, with a focus on cold environments. The thermal and charging systems under consideration are modelled, including a coolant heater and heat pump. A problem formulation that includes thermal management, charging, and charge point optimisation is presented as a non-linear, mixed integer optimal control problem. The objective of the optimisation problem is to minimise both energy delivered by the charger(s), and the time spent charging, as well as time spent on detours to and from the charging locations. This problem is then solved numerically and simulations are performed to evaluate the performance in terms of energy consumption and time spent.

The results indicate that the use of a heat pump, that allows for heat transfer from the electric drivetrain components into the cabin compartment, can reduce both energy consumption and total trip time. Energy consumption is reduced by up to 19.4% in cases where both time and energy are prioritised. In cases where mainly time is minimised, the combined time spent charging and travelling to and from charging stations is reduced by up to 30.6%.

Furthermore, the charge point optimisation results show a dynamic behaviour in terms of where to stop and charge along the trip. Main factors that affect the behaviour includes time and energy costs, heat pump power limits, and ambient temperature.

Keywords: Battery electric vehicles, Thermal management, Charging, Heat pump, Optimal control

Acknowledgements

First of all, we would like to acknowledge our supervisors Ahad Hamednia and Jimmy Forsman for their continuous guidance and encouragement during this thesis, which has been instrumental to our progress. Likewise, all the feedback given by industry experts and engineers from Volvo Cars has been helpful and enlightening. Our examiner Nikolce Murgovski has also been a source of high quality suggestions and ideas.

We also want to thank our close friends and family for their support and encouragement.

Victor Hanson & Jiaming Zhao, Gothenburg, June 2022

List of Acronyms

Below is the list of acronyms that have been used in this thesis in alphabetical order:

AC	Air Conditioning
BEV	Battery Electric Vehicle
COP	Coefficient of Performance
ED	Electric Drivetrain
EM	Electric Machine
EV	Electric Vehicle
HP	Heat Pump
HVAC	Heating Ventilation Air Conditioning
HVCH	High Voltage Coolant Heater
MPC	Model Predictive Control
PE	Power Electronics
PHEV	Plug-in Hybrid Electric Vehicle
SoC	State of Charge

Nomenclature

Below is the nomenclature of symbols that have been used in this thesis, in order of appearance.

P_{aux}	Auxiliary electrical power
$\dot{Q}_{\text{ed}}$	Electric drivetrain heat transfer
P_{ed}	Electric drivetrain electrical power
$\eta_{\text{ed}}^{\text{Q}}$	ED heat to coolant efficiency
$\eta_{\text{ed}}^{\text{e}}$	ED electric to mechanical power efficiency
$\dot{Q}_{\text{hvch}}^{\text{c}}$	HVCH heat transfer to cabin compartment
$P_{\text{hvch}}^{\text{c}}$	HVCH electrical power for cabin heating
$\eta_{\text{hvch}}^{\text{c}}$	HVCH electrical power to cabin compartment heat efficiency
$\dot{Q}_{\text{hvch}}^{\text{b}}$	HVCH heat transfer to battery loop
$P_{\text{hvch}}^{\text{b}}$	HVCH electrical power for battery heating
$\eta_{\text{hvch}}^{\text{b}}$	HVCH electrical power to battery heat efficiency
$\dot{Q}_{\text{hp}}^{\text{b}}$	HP heat transfer from battery loop
COP_{hp}	HP coefficient of performance
P_{hp}	HP electrical compressor power
T_{b}	Battery temperature
$\dot{Q}_{\text{hp}}^{\text{c}}$	HP heat transfer to cabin compartment
$\dot{Q}_{\text{c}}$	Cabin compartment heat transfer demand
T_{amb}	Ambient temperature
$\dot{Q}_{\text{hvac}}$	AC heat transfer from battery loop
P_{hvac}	AC compressor electrical power
COP_{hvac}	AC coefficient of performance
m_{b}	Battery mass
c_{p}	Battery specific heat capacity
$\dot{Q}_{\text{joule}}$	Heat transfer from Joule heating of battery internal resistance
R_{b}	Battery internal resistance

U_{OC}	Battery open-circuit voltage
P_{b}	Battery electrical power before joule losses
v	Vehicle speed
P_{grid}	Charger electrical power
$\dot{Q}_{\mathrm{pass}}$	Passive heat transfer of battery loop
$\dot{Q}_{\mathrm{act}}$	Active heat transfer of battery loop
$\dot{Q}_{\mathrm{b}}^{\mathrm{drv}}$	Battery heat transfer while driving
$\mathbf{x}_{\mathrm{drv}}$	States vector while driving
$\mathbf{u}_{\mathrm{drv}}$	Control signals vector while driving
s	Distance
c_{b}	Battery charge capacity
f_{drv}	Driving dynamics function
s_0	Distance at the start of trip
s_f	Distance at the end of trip
$\dot{Q}_{\mathrm{b}}^{\mathrm{chg}}$	Battery heat transfer while charging
τ^i	Normalised charging time at charge stop i
$t^{\mathrm{chg},i}$	Total charging time at charge stop i
i	Charge stop index
N_{chg}	The set of available charge stops
n	Label of last charge stop
$\mathbf{x}_{\mathrm{chg}}^{\mathrm{i}}$	State vector for charge stop i
$\mathbf{u}_{\mathrm{chg}}^{\mathrm{i}}$	Control signal vector for charge stop i
f_{chg}^i	Charging dynamics function
J_{chg}	Charging objective term
C_{t}	Penalty factor for charging time
C_{e}	Penalty factor for energy
J_{detour}	Detour objective term
C_{s}	Penalty factor for detour
c_{i}	Binary optimisation variable for charge stop i
$s^{\mathrm{chg},i}$	Distance at charge stop i
SoC^{detour}	SoC reduction related to detours

Contents

List of Figures

List of Tables

1
Introduction

Electric vehicles (EVs) have gained a major recognition over the past decade, due to their higher efficiency, lower local pollution and lower running costs, compared to internal combustion engine vehicles. With these benefits in mind, several governing bodies are considering zero- and low-emission technology adoption within the transportation sector, such as EVs, as an important step for further reduction of greenhouse emissions. As an example, the European commission is proposing strengthened performance standards for CO2 emissions of new passenger cars and light duty vehicles, where EVs are positioned as a technology that can meet these new standards [7]. In lieu of these developments, vehicle manufacturers that previously developed internal combustion engine vehicles are investing heavily in EV research and development, with some of them planning to only sell EVs in the near future [3].

In terms of EV technologies, the most common type of EV today is the battery electric vehicle (BEV). These vehicles, as the name implies, use an on-board battery for energy storage. Compared to other EV technologies such as hydrogen fuel cells, BEVs can readily be charged at any location where electricity is available. This enables BEVs to be charged using anything from common domestic outlets, to purpose-built fast-charging stations. However, with the limited energy density of today's lithium-ion batteries commonly used in BEVs, the range is generally shorter than most internal combustion engine vehicles.

The limited range of BEVs increases the dependence on fast, reliable, and efficient charging, especially for longer trips that can be two, three, or more times longer than the vehicles range. When planning such a trip, many questions need to be answered: At what charging station(s) should you stop? For how long should you charge at each stop? Is it better to stop once and charge for a long time, or stop multiple times and charge for a shorter time at each stop?

Tools for planning trips with BEVs that exist today are able to answer these questions without much effort from the user. Examples include the built-in navigation unit of some BEVs, or web-based tools such as [1]. These tools provide a route plan that includes information about charging stops and for how long each of them should last. However, the information that these tools use for determining how and where to charge is often based on assumptions and simplifications about the vehicle's charging performance and efficiency, leading to sub-optimal solutions in terms of energy and/or total trip time.

Charging performance of a BEV, often measured in charging time required to reach a given state of charge (SoC), depends on many factors. One factor that can have a major impact on charging time is the temperature of the battery, where too cold or too hot temperatures will lengthen the charging time significantly. Therefore, to guarantee fast and safe charging, vehicle manufacturers include thermal management systems that, much like the systems used for cabin compartment climatisation, aim to maintain the battery temperature within acceptable limits.

The complexity and feature-sets of the thermal management systems in BEVs vary, but the more advanced systems often include resistive heating elements, heat pumps, and electronically controlled valves. To allow these systems to meet demands on cabin compartment climatisation and battery thermal requirements, while being as energy efficient as possible, a control strategy is needed. This control strategy needs to strike a balance between temperature regulation performance and energy consumption, both in extreme cold and hot ambient temperatures.

This thesis proposes a problem formulation that includes thermal management as well as charging and provides the optimal solution that minimises energy consumption and/or travel time.

1.1 Research Questions

The main research questions in this thesis are:

1. How can an algorithm be developed that captures optimal thermal management and charging of a BEV during driving and charging, on trips that are longer than the vehicle's range?
2. What are the benefits of including a heat pump in the thermal management system?
3. Given charging charging possibilities along a route, how can the charging locations be chosen optimally in order to balance time and energy cost?

1.2 Scope

The scope of this thesis can be summarised as follows:

- A drive-cycle based on real-world data is used for simulations, with speed and traction power given.
- The thermal management system is pre-defined in terms of available features and layout.
- Only heating of the cabin compartment is considered, not cooling.

1.3 Related Work

Driving and charging optimisation of BEVs is considered in [6], where dynamic programming is used to find global time optimality of driving and charging. The

optimisation variables include the speed of the vehicle, where to charge, as well as how much energy should be charged at each stop.

In [14], a framework for simulations of BEV thermal management systems is developed and tested in different case studies. Performance in terms of driving range is compared across different ambient temperatures, as well as different cabin and battery temperature set-points.

What effect different thermal management system capabilities can have on a BEV's energy efficiency and range is illustrated in [5]. This work uses a Fiat 500e BEV from 2015 as a baseline for their investigation. The original thermal management system in that vehicle is not capable of capturing waste heat from the electric drivetrain for cabin heating; it is only possible to dissipate it to the ambient environment. This is compared with a different system where waste heat can be used for cabin heating using a heat pump. Bench-test calibrated models suggest that a 15% to 18% improvement in vehicle range is reasonable to expect when a heat pump is included.

A comparative study [15] that investigates different thermal management systems for BEVs over long driving cycles, found that a system that allows for waste heat recovery performed 13.5-15% better in terms of driving range in temperatures of -10 to -20°C.

Using online optimal control for an eco-driving supervisor, with a long look-ahead horizon, is investigated in [9]. Efforts are made to be able to run the optimisation in an online, real-time fashion for improved disturbance rejection, with limited computational resources.

Another work [11] investigates the use of model predictive control (MPC) methods to optimise the thermal management of a plug-in hybrid electric vehicle (PHEV) for providing 5% reduction in cooling energy use in real-world testing, compared to a state-machine based control system.

1.4 Thesis Outline

Firstly, chapter 2 addresses thermal and electrical system modelling. Secondly, the problem of achieving optimal thermal management and charging is formulated as a constrained optimisation problem defined in chapter 3. Thirdly, the proposed problem is solved numerically and analysed in terms of energy, charging time, and ambient temperature in chapter 4, with a focus on cold ambient temperatures. Lastly, chapter 5 discusses the results, forms a conclusion, and ends with suggestions for future work.

2
Modelling

In this chapter, a brief introduction to key BEV drivetrain components is given. For the remainder of the chapter, the models used to describe the thermal management system as well as the electrical system are presented.

2.1 Vehicle Modelling

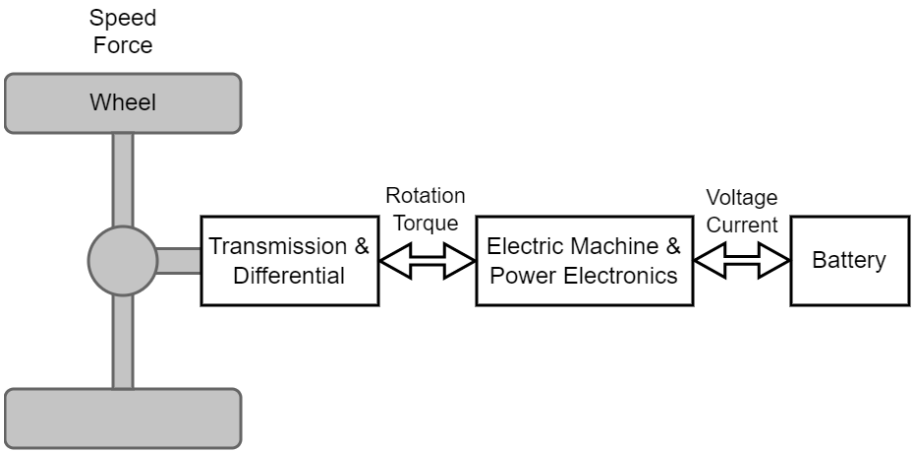

Figure 2.1: Overview of the electric drivetrain components. The battery provides electrical power for the power electronics and electric machine, which is converted to angular velocity and torque. By the use of a transmission and differential gear, the rotation and torque is transferred to the wheels which provide vehicle speed and traction force.

The main components of the electric drivetrain (ED) are the battery, the electric machine and power electronics, the transmission and differential gears, and finally the wheels. The relationship between these components are illustrated in Figure 2.1.

Multiple different forces act on a vehicle in motion, including aerodynamic drag, rolling resistance, and forces related to climbing or descending slopes. By combining these forces with the traction force delivered by the electric drivetrain, the net force acting on the vehicle body can be calculated. Furthermore, by applying Newton's second law of motion, the acceleration of the vehicle can be determined for a given vehicle mass and a given set of forces.

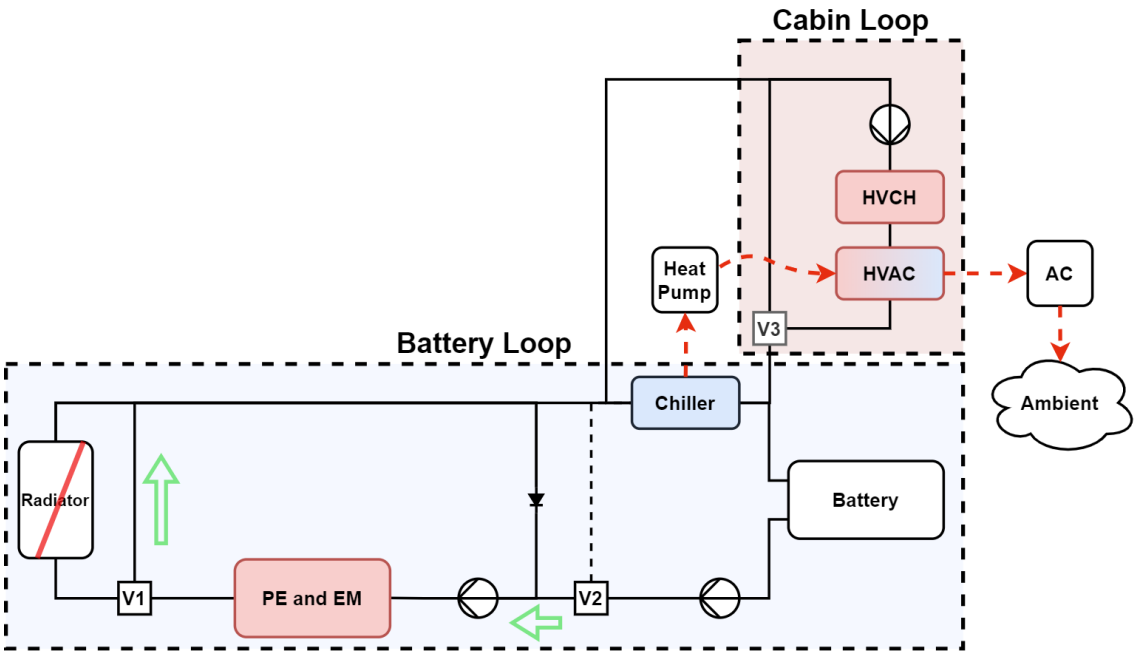

Figure 2.2: Complete thermal system overview. The battery loop and cabin loop are subsystems that contain different heat sinks and sources. Heat exchange between the two subsystems is facilitated by valve 3 (V3) and the heat pump.

Instead of modelling the vehicle dynamics as described above, to determine what traction force or power is needed to e.g. maintain a fixed speed, the traction power demand posed by the driver or by a separate system is supplied as a trajectory input. This trajectory describes the expected average traction power demand for the entire driving cycle, over a number of segments. Likewise, the vehicle speed is given for each segment of the drive cycle.

For an example of how a longitudinal vehicle model can be formulated, see [8].

2.2 Thermal and Electrical Modelling

In order to describe how the temperature of the battery changes over time, a model of the thermal management system is needed. Figure 2.2 illustrates the thermal managements system under consideration in this thesis. It consists of two coolant loops, the battery and the cabin loop, which can be considered as two separate subsystems, made up of different components.

Each relevant component of the thermal management system and electrical system is introduced and modelled for the remainder of this section. Furthermore, the key simplifications and assumptions made are highlighted. This thermal and electrical system model has been designed as a high-level, simplified model, that can be used to make high-level decisions for how the thermal management system is controlled. Since the SoC depends on the amount of energy stored in the battery, it is also necessary to model key parts of the electrical system.

For an example of a more comprehensive thermal model of an EV, see [4].

2.2.1 Valves

The thermal management system in question has a radiator, as shown in Figure 2.2, that can be used to cool down the battery loop using the ambient air. For simplicity, this radiator is not considered in this model. Thus valve one, marked as "V1" in Figure 2.2, is always in the bypass position, meaning that no coolant flows through the radiator.

Likewise, valve two (V2) is fixed in the "big loop" mode, meaning that the ED components are always part of the same loop as the battery. For cold climate operation, the heat from the ED components can be seen as a resource for heating of the battery and/or the cabin compartment. Thus fixing valve 2 in this mode ensures that the heat from the ED components is always available for heating of the battery, cabin compartment, or both. It is worth noting that in warm climate operation, this simplification is not desirable, since the heat from the ED components may cause excessive heating of the battery, beyond operating limits. In those scenarios, it is most likely desirable to separate the ED components from the battery, in order to cool the ED components using the radiator and, if needed, cool the battery using the heat pump (HP) and/or air conditioning (AC) system.

To allow for heat from the high voltage coolant heater (HVCH) to be used for heating of the battery, valve three (V3) can be used. Depending on the desired amount of cabin and battery heating, this valve can be adjusted to accommodate only cabin heating, only battery heating, or a mix of both. In this thesis the control of this valve is assumed to be done by a separate system that makes sure that the desired amount of cabin and battery heating using the HVCH is always met.

2.2.2 Coolant and Pumps

Transportation of heat amongst the different components within each loop is done using coolant, which is circulated using multiple pumps. The coolant is considered to be an ideal heat carrier in the sense that there is no delay between heat being applied to e.g. the battery loop and the temperature rising in the battery. Losses from the coolant hoses to the ambient environment is also not considered and the power consumption of the coolant pumps is considered as included in the auxiliary power consumption P_{aux}.

2.2.3 Electric Drivetrain

The main source of passive heat in this system is the electric drivetrain components, where the two main heat generating components are the electric machine (EM) and the power electronics (PE) that are used to drive the EM. Heat transfer from the

electric drivetrain is calculated as

$$\dot{Q}_{\mathrm{ed}}(P_{\mathrm{ed}}(t)) = (1 - \eta^{\mathrm{e}}_{\mathrm{ed}})P_{\mathrm{ed}}(t)\eta^{\mathrm{Q}}_{\mathrm{ed}} \tag{2.1}$$

where $\eta^{\mathrm{Q}}_{\mathrm{ed}}$ is the efficiency with which the heat losses reach the coolant, $\eta^{\mathrm{e}}_{\mathrm{ed}}$ the lumped efficiency of the ED, and P_{ed} the traction power. The efficiency of the ED in terms of electrical to mechanical power will in practice vary depending on the operating point, but for simplicity a constant efficiency is used as an approximation.

2.2.4 Coolant Heater

For introducing supplementary heat into the overall thermal system, the high voltage coolant heater is used. Primarily, it can be used to provide heat for the cabin compartment. However, the HVCH can also be used for heating of the battery, since valve 3 (V3) in Figure 2.2 allows for heat exchange between the cabin loop and the battery loop, as previously mentioned. The heat provided by the HVCH is given as

$$\dot{Q}^{\mathrm{c}}_{\mathrm{hvch}}(P^{\mathrm{c}}_{\mathrm{hvch}}(t)) = \eta^{\mathrm{c}}_{\mathrm{hvch}}P^{\mathrm{c}}_{\mathrm{hvch}}(t) \tag{2.2}$$

$$\dot{Q}^{\mathrm{b}}_{\mathrm{hvch}}(P^{\mathrm{b}}_{\mathrm{hvch}}(t)) = \eta^{\mathrm{b}}_{\mathrm{hvch}}P^{\mathrm{b}}_{\mathrm{hvch}}(t) \tag{2.3}$$

where $\dot{Q}^{\mathrm{c}}_{\mathrm{hvch}}$ is the heat provided for cabin heating, $\eta^{\mathrm{c}}_{\mathrm{hvch}}$ is the efficiency of the HVCH for cabin heating, and $P^{\mathrm{c}}_{\mathrm{hvch}}$ is the electrical power used for cabin heating. Similarly, $\dot{Q}^{\mathrm{b}}_{\mathrm{hvch}}$, $\eta^{\mathrm{b}}_{\mathrm{hvch}}$, and $P^{\mathrm{b}}_{\mathrm{hvch}}$ is the heat provided by the HVCH for battery heating, the efficiency of the HVCH for battery heating, and the electrical power used for battery heating, respectively.

The HVCH heating power is constrained by a maximum power. The sum of the power provided by the HVCH for battery heating and for cabin heating should be less than or equal to the maximum power. This can be described as

$$P^{\mathrm{max}}_{\mathrm{hvch}}(t) \geq P^{\mathrm{b}}_{\mathrm{hvch}}(t) + P^{\mathrm{c}}_{\mathrm{hvch}}(t) \tag{2.4}$$

where $P^{\mathrm{max}}_{\mathrm{hvch}}(t)$ is the maximum HVCH power.

2.2.5 Heat Pump

The second law of thermodynamics tells us that heat will only spontaneously transfer from a high temperature body to a low temperature body, not in the other direction. This is true for spontaneous processes, but by introducing work in the form of compression, a vapour-compression heat pump is able to capture thermal energy from an evaporator at a lower temperature and expel it into a condenser at a higher temperature. The process uses a refrigerant, circulated between the condenser and evaporator by a compressor, combined with an expansion valve. The work required by the heat pump compressor is in many cases half or less of the heat that is being transferred, depending on operating conditions. This makes a heat pump a more efficient alternative to resistive heating, since for resistive heating, the heat delivered

is at best equal to the electrical work provided. For a more detailed explanation of HP operation and modelling, see [13].

In this thesis, a heat pump is used to move thermal energy from the battery loop to the cabin loop. In Figure 2.2, the "chiller" represents the evaporator. The condenser is part of the heating ventilation and air conditioning (HVAC) system. This allows for waste heat and stored thermal energy from the battery to be used for cabin compartment heating. The heat removed from the battery loop by the heat pump $\dot{Q}_{\mathrm{hp}}^{\mathrm{b}}$ is described as

$$\dot{Q}_{\mathrm{hp}}^{\mathrm{b}}(COP_{\mathrm{hp}}(T_{\mathrm{b}}(t)), P_{\mathrm{hp}}(t)) = (COP_{\mathrm{hp}}(T_{\mathrm{b}}(t)) - 1)P_{\mathrm{hp}}(t) \tag{2.5}$$

where COP_{hp} is the coefficient of performance (COP) for the heat pump and P_{hp} is HP compressor electrical power. As a coefficient indicating the ratio between the heat power provided for heating and the electrical power supplied to the compressor, COP_{hp} is proportional to the battery temperature T_{b}. When the COP is greater than one, it is beneficial to use the HP instead of the HVCH, since more heat is delivered to the cabin compartment than the amount of compression work done by the compressor. If the COP is equal to one, the HP is only on-par with the HVCH.

The heat power provided for cabin heating by the HP is

$$\dot{Q}_{\mathrm{hp}}^{\mathrm{c}}(COP_{\mathrm{hp}}(T_{\mathrm{b}}(t)), P_{\mathrm{hp}}(t)) = COP_{\mathrm{hp}}(T_{\mathrm{b}}(t))P_{\mathrm{hp}}(t)\ . \tag{2.6}$$

The heat pump compressor power is constrained by a maximum power denoted $P_{\mathrm{hp}}^{\max}(t)$

2.2.6 Cabin Compartment Heating

Both the heat pump and the HVCH are able to provide cabin compartment heating, as mentioned in the previous sections. The relationship between cabin compartment heat demand $\dot{Q}_{\mathrm{c}}$ and the heat provided is

$$\dot{Q}_{\mathrm{c}}(T_{\mathrm{amb}}(t)) = \dot{Q}_{\mathrm{hp}}^{\mathrm{c}}(\cdot) + \dot{Q}_{\mathrm{hvch}}^{\mathrm{c}}(\cdot) \tag{2.7}$$

where the cabin compartment heat demand is a piece-wise linear function, inversely proportional to the ambient temperature T_{amb}. This formulation means that the cabin heat demand is met at all times, either by the HP, the HVCH, or by a combination of both.

2.2.7 HVAC AC Cooling

One part of HVAC is the air conditioning system, that can be used to cool and de-humidify the cabin compartment. This system is in many ways similar to the heat pump presented previously, with the key difference that heat is moved from the cabin loop to the ambient air.

Since cooling of the cabin compartment is not considered in this thesis, the only use for the AC system is to cool the battery in cases where excess heat needs to be removed from the system. For simplicity, the heat that is removed by the AC system is therefore removed directly from the battery loop in the model, rather than from the cabin loop. The heat removed from the battery loop by the AC system is

$$\dot{Q}_{\text{hvac}}(P_{\text{hvac}}(t)) = P_{\text{hvac}}(t)COP_{\text{hvac}} \tag{2.8}$$

which is similar to the equation used for the HP. Here COP_{hvac} is the ratio between the heat removed from the battery loop and the AC compressor power, where $P_{\text{hvac}}^{\max}(t)$ is the maximum AC compressor power constraint. For simplicity, COP_{hvac} is considered to be constant.

2.2.8 Battery

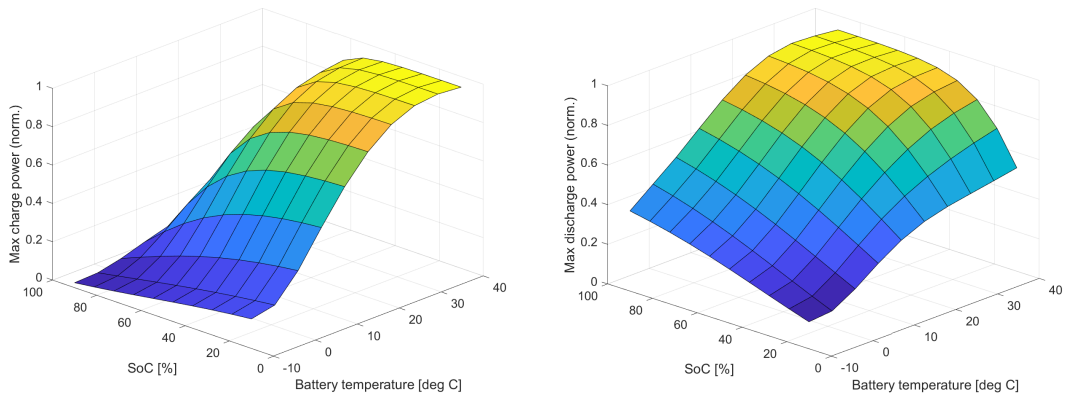

(a) Charge power limits. **(b)** Discharge power limits.

Figure 2.3: Normalised battery power limits over battery temperature and SoC.

In order to minimise charging time, the charging power should be maximised. The main limiting factors on charging power are the charger and the battery, where the charger has a maximum rated power output that cannot be exceeded, and the battery has a maximum charge power that depends on battery temperature and SoC. The functions used to describe the relationship between battery temperature, SoC, and maximum charge or discharge power of the battery are depicted in Figure 2.3. Maximum charging power is at its peak when SoC is low while battery temperature is high, and drops as SoC increases and temperature decreases. On the contrary, the highest maximum discharge power is observed when both SoC and battery temperature are high, and drops as they decrease. For fast charging, the maximum charge power is clearly what is important. However, while driving, the maximum discharge power is also of interest since it can limit traction power.

The battery is modelled as a uniform thermal mass. This is a simplification since, in reality, the battery is a battery *pack*, consisting of many cells. These cells heat

up and cool down slightly differently from one another, in part due to differences in internal resistance and/or uneven external heat exchange from the coolant or ambient. The battery temperature considered in this project can thus be seen as the average temperature across all the individual cells that make up the battery. How the temperature of the battery T_b changes over time can be formulated as

$$\begin{aligned}\dot{T}_\mathrm{b}(t) = \frac{1}{m_\mathrm{b} c_\mathrm{p}}(&\dot{Q}_\mathrm{ed}(P_\mathrm{ed}(t)) + \dot{Q}_\mathrm{joule}(R_\mathrm{b}(T_\mathrm{b}(t)), P_\mathrm{b}(t), U_\mathrm{OC}(SoC(t))) + \dot{Q}^\mathrm{b}_\mathrm{hvch}(P^\mathrm{b}_\mathrm{hvch}(t)) \\ &- \dot{Q}^\mathrm{b}_\mathrm{hp}(COP_\mathrm{hp}(T_\mathrm{b}(t)), P_\mathrm{hp}(t)) - \dot{Q}_\mathrm{hvac}(P_\mathrm{hvac}(t)) - \dot{Q}_\mathrm{amb}(T_\mathrm{b}(t), T_\mathrm{amb}(t), v(t)))\end{aligned} \tag{2.9}$$

where m_b is the mass of the battery and c_p is the specific heat capacity of the battery. Furthermore, $\dot{Q}_\mathrm{ed}$, $\dot{Q}_\mathrm{joule}$, $\dot{Q}^\mathrm{b}_\mathrm{hvch}$, $\dot{Q}^\mathrm{b}_\mathrm{hp}$, and $\dot{Q}_\mathrm{hvac}$ are heat losses from the electric drivetrain, joule heating from resistive losses within the battery, heat from the coolant heater for battery heating, heat removed by the heat pump, and heat removed by the HVAC AC system, respectively. The heat transfer term $\dot{Q}_\mathrm{amb}$ denotes the heat that is either absorbed from or released to the ambient environment through the battery casing. This is described by a non-linear function dependent on battery temperature $T_\mathrm{b}(t)$, ambient temperature $T_\mathrm{amb}(t)$, and vehicle speed $v(t)$.

The battery electrical power P_b is described by

$$\begin{aligned}P_\mathrm{b}(t) = R_\mathrm{b}(T_\mathrm{b}(t))\frac{P_\mathrm{b}(t)^2}{U^2_\mathrm{OC}(SoC(t))} + P_\mathrm{ed}(t) + P^\mathrm{b}_\mathrm{hvch}(t) + P^\mathrm{c}_\mathrm{hvch}(t) + P_\mathrm{aux}(t) + P_\mathrm{hp}(t) \\ + P_\mathrm{hvac}(t) - P_\mathrm{grid}(t)\end{aligned} \tag{2.10}$$

where P_ed, $P^\mathrm{b}_\mathrm{hvch}$, $P^\mathrm{c}_\mathrm{hvch}$, P_aux, P_hp, P_hvac, and P_grid are traction power, coolant heater power for battery heating, coolant heater power for cabin heating, auxiliary power, heat pump compressor power, HVAC AC compressor power, and power from the charger, respectively. The battery open-circuit voltage U_OC is a non-linear function of SoC, where the voltage increases with higher SoC. R_b is the internal resistance of the battery, which is a non-linear function of battery temperature where increasing battery temperature results in lower internal resistance.

Among the terms influencing the heat transfer within the battery, the Joule heat generated by battery internal resistance, based on Joule's first law, is calculated as

$$\dot{Q}_\mathrm{joule}(R_\mathrm{b}(T_\mathrm{b}(t)), P_\mathrm{b}(t), U_\mathrm{OC}(SoC(t))) = R_\mathrm{b}(T_\mathrm{b}(t))\frac{P_\mathrm{b}(t)^2}{U^2_\mathrm{OC}(SoC(t))}\ . \tag{2.11}$$

2.2.9 Summary

To understand how the battery temperature changes during driving and charging, the heat transfer can be divided into passive heating and active heating. In this section, different heat transfer branches are summarised for the simplicity of further

use in later chapters.

The passive heat transfer can be summarised as

$$\begin{aligned}&\dot{Q}_{\text{pass}}(P_{\text{ed}}(t), R_{\text{b}}(T_{\text{b}}(t)), P_{\text{b}}(t), U_{\text{OC}}(SoC(t)), T_{\text{b}}(t), T_{\text{amb}}(t), v(t))\\ =&\dot{Q}_{\text{ed}}(P_{\text{ed}}(t)) + \dot{Q}_{\text{joule}}(R_{\text{b}}(T_{\text{b}}(t)), P_{\text{b}}(t), U_{\text{OC}}(SoC(t))) - \dot{Q}_{\text{amb}}(T_{\text{b}}(t), T_{\text{amb}}(t), v(t))\end{aligned} \tag{2.12}$$

where heat sources are the losses from the electric drivetrain $\dot{Q}_{\text{ed}}$ and the Joule losses within the battery $\dot{Q}_{\text{joule}}$. Heat is also dissipated from the battery to the ambient environment $\dot{Q}_{\text{amb}}$. It is worth mentioning that the ED heat loss only exists during driving.

The actively generated and lost heat, $\dot{Q}_{\text{act}}$, can be described as

$$\begin{aligned}&\dot{Q}_{\text{act}}(P^{\text{b}}_{\text{hvch}}(t), COP_{\text{hp}}(T_{\text{b}}(t)), P_{\text{hp}}(t), P_{\text{hvac}}(t))\\ =&\dot{Q}^{\text{b}}_{\text{hvch}}(P^{\text{b}}_{\text{hvch}}(t)) - \dot{Q}^{\text{b}}_{\text{hp}}(COP_{\text{hp}}(T_{\text{b}}(t)), P_{\text{hp}}(t)) - \dot{Q}_{\text{hvac}}(P_{\text{hvac}}(t))\end{aligned} \tag{2.13}$$

where the only active heat source for the battery is HVCH $\dot{Q}^{\text{b}}_{\text{hvch}}$, which applies to both driving and charging. The active heat loss includes the heat extracted by the heat pump $\dot{Q}^{\text{b}}_{\text{hp}}$ and the heat removed through HVAC system $\dot{Q}_{\text{hvac}}$. Similarly, the formulation of the heat loss between battery and ambient varies with driving or charging since one component is directly related to the vehicle speed $v(t)$.

3

Optimal Thermal Management and Charging

At the start of this chapter, an introduction to the scenario considered in this thesis is described. For the remainder of the chapter, the problem formulation of driving mode, charging mode, and combination are analysed respectively, where charge point optimisation is also included.

3.1 Scenario

In the scenario of this thesis, a BEV starts a long trip with a given SoC and battery temperature. The distance of the trip is longer than the range of the vehicle, necessitating charging along the trip. Multiple charge points are available along the trip, but there is no strict need to stop at each of them to complete the trip. A balance between travelling time and energy efficiency needs to be found. This scenario is demonstrated in Figure 3.1.

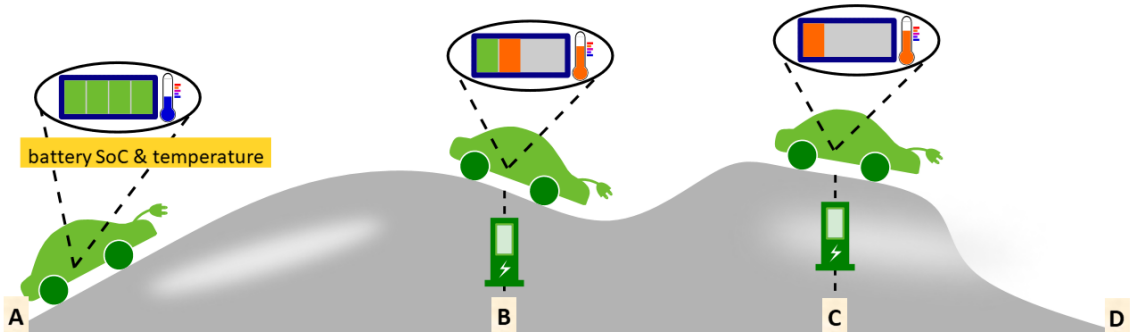

Figure 3.1: Problem scenario involving a trip longer than the vehicle's range, with multiple different charging opportunities available. The trip starts at position A with a given SoC and battery temperature. As the vehicle drives along the route, the battery SoC and temperature changes. Positions B and C represent opportunities to charge along the trip. The trip is finished once the vehicle reaches position D. Modified and used with permission from [10].

3.2 Problem Formulation

The following section covers the sub-problems of driving, charging, and charge point optimisation, before combining the problems into a condensed problem formulation.

3.2.1 Driving Mode

For the driving mode, according to the battery heat transfer analysis in chapter 2, the heat balance during driving can be described as

$$\dot{Q}_{\mathrm{b}}^{\mathrm{drv}}(\cdot) = \dot{Q}_{\mathrm{pass}}(\cdot) + \dot{Q}_{\mathrm{act}}(\cdot) \ . \tag{3.1}$$

Driving distance s is chosen as the independent variable in the driving mode. The dynamics include battery temperature and battery state of charge, and control signals consist of HVCH power for battery heating, battery power, heat pump and HVAC cooling compressor powers. Two vectors are defined for states and controls as

$$\mathbf{x}_{\mathrm{drv}}(s) = \begin{bmatrix} T_{\mathrm{b}}^{\mathrm{drv}}(s) \\ SoC^{\mathrm{drv}}(s) \end{bmatrix}, \ \mathbf{u}_{\mathrm{drv}}(s) = \begin{bmatrix} P_{\mathrm{hvch}}^{\mathrm{b,drv}}(s) \\ P_{\mathrm{b}}^{\mathrm{drv}}(s) \\ P_{\mathrm{hp}}^{\mathrm{drv}}(s) \\ P_{\mathrm{hvac}}^{\mathrm{drv}}(s) \end{bmatrix}. \tag{3.2}$$

To reformulate the dynamics with respect to driving distance s, the necessary relationship between driving time dependant and driving distance dependent dynamics can be described as

$$\frac{d\mathbf{x}_{\mathrm{drv}}(t)}{dt \ v(s)} = \frac{d\mathbf{x}_{\mathrm{drv}}(s)}{ds} \ . \tag{3.3}$$

According to equation (3.3), the dynamics during driving can be described as

$$\frac{dT_{\mathrm{b}}^{\mathrm{drv}}(s)}{ds} = \frac{1}{c_{\mathrm{p}} m_{\mathrm{b}} v(s)} (\dot{Q}_{\mathrm{b}}^{\mathrm{drv}}(\cdot)) \tag{3.4a}$$

$$\frac{dSoC^{\mathrm{drv}}(s)}{ds} = -\frac{P_{\mathrm{b}}^{\mathrm{drv}}(s)}{U_{\mathrm{OC}}(SoC^{\mathrm{drv}}(s)) \epsilon_{\mathrm{b}} v(s)} \tag{3.4b}$$

where c_{p}, m_{b}, and ϵ_{b} stand for the specific heat capacity of the battery, battery mass, and battery charge capacity, respectively. The negative sign is added to the expression of dynamics for battery SoC since the battery power is defined as positive when power is being supplied by the battery, in which case the SoC is decreasing.

The driving dynamics from equation (3.4) can be represented by a vector valued function f_{drv} as

$$\frac{d\mathbf{x}_{\mathrm{drv}}(s)}{ds} = f_{\mathrm{drv}}(\mathbf{x}_{\mathrm{drv}}(s), \mathbf{u}_{\mathrm{drv}}(s), s) \ . \tag{3.5}$$

The power balance relationship during driving is described as

$$P_{\mathrm{b}}^{\mathrm{drv}}(s) = (\frac{P_{\mathrm{b}}^{\mathrm{drv}}(s)}{U_{\mathrm{OC}}(SoC^{\mathrm{drv}}(s))})^2 R_{\mathrm{b}}(T_{\mathrm{b}}^{\mathrm{drv}}(s)) + P_{\mathrm{ed}}^{\mathrm{drv}}(s) + P_{\mathrm{hvch}}^{\mathrm{b,drv}}(s) + P_{\mathrm{hvch}}^{\mathrm{c,drv}}(s) + P_{\mathrm{hvac}}^{\mathrm{drv}}(s) + P_{\mathrm{hp}}^{\mathrm{drv}}(s) + P_{\mathrm{aux}}^{\mathrm{drv}}(s) \ . \tag{3.6}$$

In this thesis, the vehicle speed is a given value, meaning that a time cost associated with driving time is unnecessary, since the driving time is constant. Furthermore, the vehicle is expected to have to stop and charge at least once during the trip, meaning that there is no need to have a separate energy cost for driving, because the energy used while driving is reflected in the amount of energy that needs to be charged.

The initial and general constraints on battery temperature and SoC while driving are described as

$$T_{\mathrm{b}}^{\mathrm{drv}}(s_0) = T_{\mathrm{b}}^{\mathrm{init}}, \tag{3.7a}$$
$$SoC^{\mathrm{drv}}(s_0) = SoC^{\mathrm{init}} \tag{3.7b}$$
$$T_{\mathrm{b}}^{\mathrm{drv}}(s_{\mathrm{f}}) \geq T_{\mathrm{b}}^{\mathrm{end}} \tag{3.7c}$$
$$SoC^{\mathrm{drv}}(s_{\mathrm{f}}) \geq SoC^{\mathrm{end}} \tag{3.7d}$$

where s_0 and s_{f} are the initial and final travelling distance of the whole driving cycle. $T_{\mathrm{b}}^{\mathrm{init}}$ and SoC^{init} are given initial starting state values. $T_{\mathrm{b}}^{\mathrm{end}}$ and SoC^{end} represent constraints on the final values of battery temperature and SoC, respectively.

3.2.2 Charging Mode

In the charging mode, the heat transfer balance is described as

$$\dot{Q}_{\mathrm{b}}^{\mathrm{chg}}(\cdot) = \dot{Q}_{\mathrm{pass}}(\cdot) + \dot{Q}_{\mathrm{act}}(\cdot) \ . \tag{3.8}$$

It is worth noting that, compared to the driving mode described in the previous section, the battery heat transfer components when charging do not include the heat loss from ED because no traction power is supplied when stationary. Similarly, for the ambient heat loss $\dot{Q}_{\mathrm{amb}}^{\mathrm{chg}}$, there is only a dependence on ambient and battery temperature, since the vehicle speed is zero while charging.

In charging mode, charging time at each charge point is an optimisation variable. This means that the charging time t is not a useful independent variable, since the

discretisation step would vary with the charging time, complicating the implementation. Furthermore, due to the fact that the BEV is stationary while charging, travel distance s cannot be used as an independent variable. To solve these issues, the normalised charging time at each charge point τ^i is chosen as the independent variable, where i is an integer belongs to the label list of all n available charging points along the trip. A charge session starts with τ equal to zero, and ends when τ reaches one. The relationship among the normalised charging time τ^i, the total charging time $t^{\mathrm{chg},i}$, and the charging time at the current moment t is described as

$$\frac{1}{d\tau^i} = \frac{t^{\mathrm{chg},i}}{dt},\ i \in N_{\mathrm{chg}} = \{1, 2, 3, ..., n\}\ . \tag{3.9}$$

Even though the normalised charging time τ is used as the independent variable during different charging sessions, the dynamics still include the battery temperature and SoC, and control signals consist of HVCH power for battery heating, battery power, heat pump compressor power, and HVAC cooling compressor power. Dynamics and controls at different charging stops are defined as

$$\mathbf{x}^i_{\mathrm{chg}}(\tau^i) = \begin{bmatrix} T_{\mathrm{b}}^{\mathrm{chg},i}(\tau^i) \\ SoC^{\mathrm{chg},i}(\tau^i) \end{bmatrix},\ \mathbf{u}^i_{\mathrm{chg}}(\tau^i) = \begin{bmatrix} P_{\mathrm{hvch}}^{\mathrm{b,chg},i}(\tau^i) \\ P_{\mathrm{b}}^{\mathrm{chg},i}(\tau^i) \\ P_{\mathrm{hp}}^{\mathrm{chg},i}(\tau^i) \\ P_{\mathrm{hvac}}^{\mathrm{chg},i}(\tau^i) \end{bmatrix}. \tag{3.10}$$

More specifically, the dynamics are described as

$$\frac{dT_{\mathrm{b}}^{\mathrm{chg},i}(\tau^i)}{d\tau^i} = \frac{t^{\mathrm{chg},i}}{c_{\mathrm{p}} m_{\mathrm{b}}} \dot{Q}_{\mathrm{b}}^{\mathrm{chg}}(\cdot) \tag{3.11a}$$

$$\frac{dSoC^{\mathrm{chg},i}(\tau^i)}{d\tau^i} = -\frac{t^{\mathrm{chg},i} P_{\mathrm{b}}^{\mathrm{chg},i}(\tau^i)}{c_{\mathrm{b}} U_{\mathrm{OC}}(SoC^{\mathrm{chg},i}(\tau^i))} \tag{3.11b}$$

where c_{p}, m_{b} and c_{b} stand for the same terms respectively as what they stand for under the driving mode.

The charging dynamics from equation (3.4) can be represented by a vector valued function f^i_{chg} as

$$\frac{d\mathbf{x}_{\mathrm{chg}}(\tau^i)}{d\tau^i} = f^i_{\mathrm{chg}}(\mathbf{x}^i_{\mathrm{chg}}(\tau^i), \mathbf{u}^i_{\mathrm{chg}}(\tau^i), \tau^i)\ . \tag{3.12}$$

In the charging mode, the cost function integrated over the normalised charging time is defined as

$$J_{\mathrm{chg}}(\cdot) = \sum_{i=1}^{n} (C_{\mathrm{t}} t^{\mathrm{chg},i} + C_{\mathrm{e}} \int_0^1 P^i_{\mathrm{grid}}(\tau^i)\ d\tau_i)\ . \tag{3.13}$$

where C_{t} and C_{e} are the penalty factors for the charging time and charging energy at each charging stop.

During charging, the power balance equation is described as

$$P^i_{\text{grid}}(\tau^i) = \left(\frac{P^{\text{chg},i}_{\text{b}}(\tau^i)}{U_{\text{OC}}(SoC^{\text{chg},i}(\tau_i))}\right)^2 R_{\text{b}}(T^{\text{chg},i}_{\text{b}}(\tau^i)) + P^{\text{b,chg},i}_{\text{hvch}}(\tau^i) + P^{\text{c,chg},i}_{\text{hvch}}(\tau^i) + P^{\text{chg},i}_{\text{hvac}}(\tau^i) + P^{\text{chg},i}_{\text{hp}}(\tau^i) + P^{\text{chg},i}_{\text{aux}}(\tau^i) - P^{\text{chg},i}_{\text{b}}(\tau^i)\ . \quad (3.14)$$

3.2.3 Charge Point Optimisation

To allow for skipping of charging stops along the trip, charge point optimisation is introduced with detour cost described as

$$J_{\text{detour}}(\cdot) = C_{\text{s}} \sum_{i=1}^{n} c_i \tag{3.15a}$$

$$c_i \in \{0, 1\} \ . \tag{3.15b}$$

From the above objective function, binary variable c_i is introduced as the optimisation variable for each possible charge stop, where a value of 0 means skipping the corresponding i^{th} charge stop, while a value of 1 stands for stopping and charging.

3.2.4 Combined Driving and Charging

In the case of the driving and charging combination, the journey starts and ends with the driving, and several charge stops are available along the trip. The start and end states between different driving and charging sessions are described as

$$T_{\text{b}}^{\text{drv}}(s_0) = T_{\text{b}}^{\text{init}}, \ SoC^{\text{drv}}(s_0) = SoC^{\text{init}} \tag{3.16a}$$

$$T_{\text{b}}^{\text{chg},i}(0) = T_{\text{b}}^{\text{drv}}(s^{\text{chg},i}), \ SoC^{\text{chg},i}(0) = SoC^{\text{drv}}(s^{\text{chg},i}) - c_i SoC^{\text{detour}} \tag{3.16b}$$

$$T_{\text{b}}^{\text{drv}}(s^{\text{chg},i+}) = T_{\text{b}}^{\text{chg},i}(1), \ SoC^{\text{drv}}(s^{\text{chg},i+}) = SoC^{\text{chg},i}(1) - c_i SoC^{\text{detour}} \tag{3.16c}$$

where the SoC reduction caused by a detour between the main route and decided charge stops, SoC^{detour}, is introduced to make the connection between driving and charging sessions more realistic, since some energy is used in order to travel to and from the charging location. $s^{\text{chg},i+}$ represents the instance when the charging is finished and the BEV leaves the charging location.

3.2.5 Complete Problem Formulation

The following problem formulation combines the sub-problems of driving, charging, and charge point optimisation into one, complete formulation.

$$\min_{\mathbf{u}_{\mathrm{drv}}(s),\mathbf{u}^i_{\mathrm{chg}}(\tau^i),t^{\mathrm{chg},i},c_i} \{J_{\mathrm{chg}}(\cdot) + J_{\mathrm{detour}}(\cdot)\} \tag{3.17a}$$

subject to:

$$c_i \in \{0,1\} \tag{3.17b}$$
$$\tau_i \in [0,1] \tag{3.17c}$$
$$\frac{d\mathbf{x}_{\mathrm{drv}}(s)}{ds} = f_{\mathrm{drv}}(\mathbf{x}_{\mathrm{drv}}(s), \mathbf{u}_{\mathrm{drv}}(s), s) \tag{3.17d}$$
$$\frac{d\mathbf{x}_{\mathrm{chg}}(\tau^i)}{d\tau^i} = f^i_{\mathrm{chg}}(\mathbf{x}^i_{\mathrm{chg}}(\tau^i), \mathbf{u}^i_{\mathrm{chg}}(\tau^i), \tau^i) \tag{3.17e}$$
$$P^{\mathrm{b}}_{\mathrm{hvch}}(\cdot) \in [0, P^{\max}_{\mathrm{hvch}}(\cdot) - P^{\mathrm{c}}_{\mathrm{hvch}}(\cdot)] \tag{3.17f}$$
$$P_{\mathrm{hvac}}(\cdot) \in [0, P^{\max}_{\mathrm{hvac}}(\cdot)] \tag{3.17g}$$
$$P_{\mathrm{hp}}(\cdot) \in [0, P^{\max}_{\mathrm{hp}}(\cdot)] \tag{3.17h}$$
$$T_{\mathrm{b}}(\cdot) \in [T^{\min}_{\mathrm{b}}(\cdot), T^{\max}_{\mathrm{b}}(\cdot)] \tag{3.17i}$$
$$SoC(\cdot) \in [SoC_{\min}(\cdot), SoC_{\max}(\cdot)] \tag{3.17j}$$
$$P_{\mathrm{b}}(\cdot) \in [P^{\min}_{\mathrm{b}}(\cdot), P^{\max}_{\mathrm{b}}(\cdot)] \tag{3.17k}$$
$$P^i_{\mathrm{grid}}(\tau_i) \in [0, c_i P^{i,\max}_{\mathrm{grid}}(\tau_i)] \tag{3.17l}$$
$$t^{\mathrm{chg},i} \in [0, c_i t^{\mathrm{chg},i\ \max}] \tag{3.17m}$$
$$T^{\mathrm{drv}}_{\mathrm{b}}(s_0) = T^{\mathrm{init}}_{\mathrm{b}},\ SoC^{\mathrm{drv}}(s_0) = SoC^{\mathrm{init}} \tag{3.17n}$$
$$T^{\mathrm{chg},i}_{\mathrm{b}}(0) = T^{\mathrm{drv}}_{\mathrm{b}}(s^{\mathrm{chg},i}),\ SoC^{\mathrm{chg},i}(0) = SoC^{\mathrm{drv}}(s^{\mathrm{chg},i}) - c_i SoC^{\mathrm{detour}} \tag{3.17o}$$
$$T^{\mathrm{drv}}_{\mathrm{b}}(s^{\mathrm{chg},i\ +}) = T^{\mathrm{chg},i}_{\mathrm{b}}(1),\ SoC^{\mathrm{drv}}(s^{\mathrm{chg},i\ +}) = SoC^{\mathrm{chg},i}(1) - c_i SoC^{\mathrm{detour}} \tag{3.17p}$$
$$SoC^{\mathrm{drv}}(s_{\mathrm{f}}) \geq SoC^{\mathrm{end}},\ T^{\mathrm{drv}}_{\mathrm{b}}(s_{\mathrm{f}}) \geq T^{\mathrm{end}}_{\mathrm{b}} \tag{3.17q}$$

This complete formulation is a mixed integer, non-linear programming (MINLP) problem, since the charge point optimisation introduces integer variables. The objective function only contains terms related to charging and charge point optimisation, not driving.

Inequality constraints in equations (3.17f-m) and (3.17q) are included for the states, coolant heater power, HVAC cooling power, heat pump power, and battery power. For the charging sessions, constraints on charger power and charging time are also included. The final values of the states are constrained by independent inequality constraints.

Equality constraints in equations (3.17n-p) are used to set the initial state values and to manage the switch from driving to charging and vice versa, including detour energy consumption that acts on the SoC.

4
Results

This chapter begins by briefly explaining the tools and setup used for simulations and continues with results.

4.1 Setup

The underlying tool used to perform the simulations is MATLAB version R2019b. CasADi [2] is used as an extension of MATLAB, to efficiently be able to translate the mathematical problem formulation into a numerical implementation, using symbolic expressions.

The solver used with CasADi is Bonmin [12], which is a general non-linear, mixed integer solver.

4.1.1 Driving Cycle

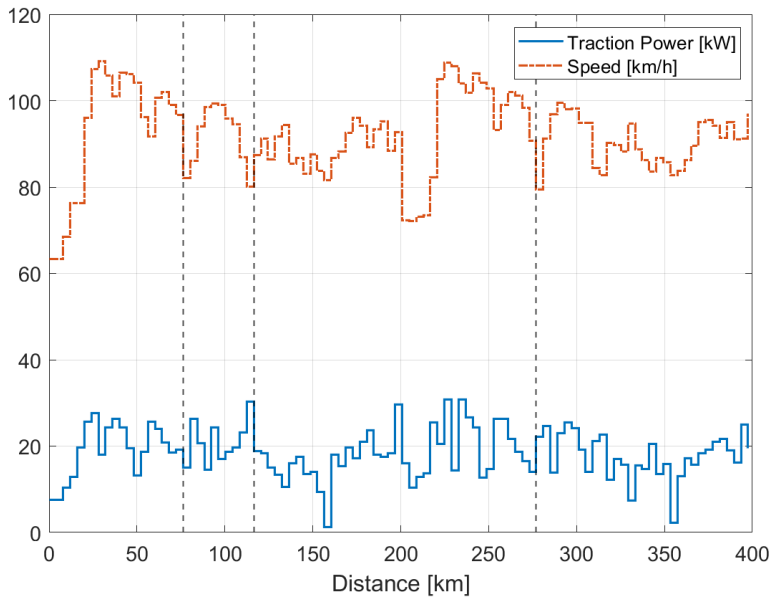

Figure 4.1: The drive cycle including the vehicle speed and traction power trajectories. Dashed vertical lines indicate available charging locations.

The drive cycle used for the simulations is about 400 km long and is based on real-world measurements. Three charging locations are available along the trip, marked by dashed vertical lines in Figure 4.1. In later figures, a solid vertical line indicates that a charging stop was performed, and a dashed line indicates that the stop was skipped.

4.1.2 Parameters

The following parameters are used for the simulations, unless otherwise noted. For these simulations, the cabin compartment heating demand is maintained at all times, including during charging.

Symbol	Value(s)	Unit	Description
T_{amb}	{-10, 0, 10}	°C	Ambient temperature.
$\eta_{\text{ed}}^{\text{Q}}$	80	%	Efficiency of heat transfer from ED to battery coolant loop.
η_{ed}	90	%	Efficiency of ED electrical to mechanical power.
$\eta_{\text{HVCH}}^{\text{b}}$	87	%	Efficiency of heat transfer from HVCH to battery coolant loop.
$\eta_{\text{HVCH}}^{\text{c}}$	95	%	Efficiency of heat transfer from HVCH to cabin compartment.
$P_{\text{HP}}^{\text{max}}$	{0, 1, 3}	kW	Maximum HP compressor electrical power.
$P_{\text{HP}}^{\text{min}}$	0	kW	Minimum HP compressor electrical power.
$P_{\text{HVAC}}^{\text{max}}$	3	kW	Maximum HVAC compressor power.
$P_{\text{HVAC}}^{\text{min}}$	0	kW	Minimum HVAC compressor power.
P_{aux}	500	W	Auxiliary electrical load.
$T_{\text{b}}^{\text{max}}$	40	°C	Maximum battery temperature.
$T_{\text{b}}^{\text{min}}$	-20	°C	Minimum battery temperature.
SoC_{max}	100	%	Maximum battery state of charge.
SoC_{min}	10	%	Minimum battery state of charge.
N_{drive}	100	steps	Number of discretisation steps for driving mode.
N_{charge}	25	steps	Number of discretisation steps for charging mode.
t_{detour}	300	s	Detour time for each charging stop.
E_{detour}	450	Wh	Detour energy for each charging stop.
C_{t}	[0.1, 10000]	SEK/h	Cost per hour of charging and detour time.
C_{e}	8.7	SEK/kWh	Cost per kWh of energy delivered by charger.
$T\text{b}^{\text{init}}$	T_{amb}	°C	Initial battery temperature.
SoC_{init}	90	%	Initial battery state of charge.

Table 4.1: Parameters used for simulations.

4.2 Charged Energy vs. Charging and Detour Time

This section compares the energy delivered by chargers to the combined detour and charging time. The time cost is varied from 0.1 to 10000 SEK/h in order to yield solutions that vary from energy optimal to time optimal.

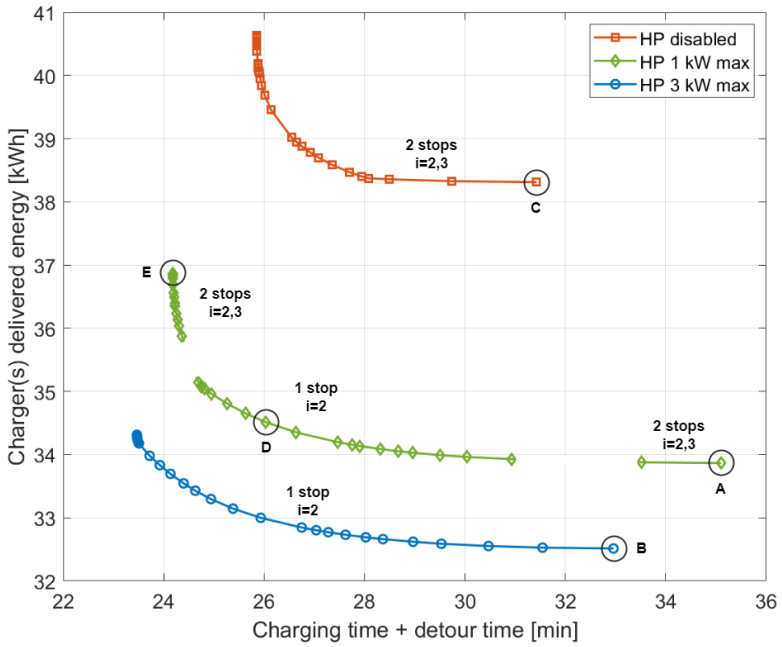

Figure 4.2: Comparison of charged energy and time spent charging combined with detour time. Heat pump is either disabled or limited to 1 or 3 kW. Ambient temperature of -10°C. Circled points A-E are investigated in detail in later sections.

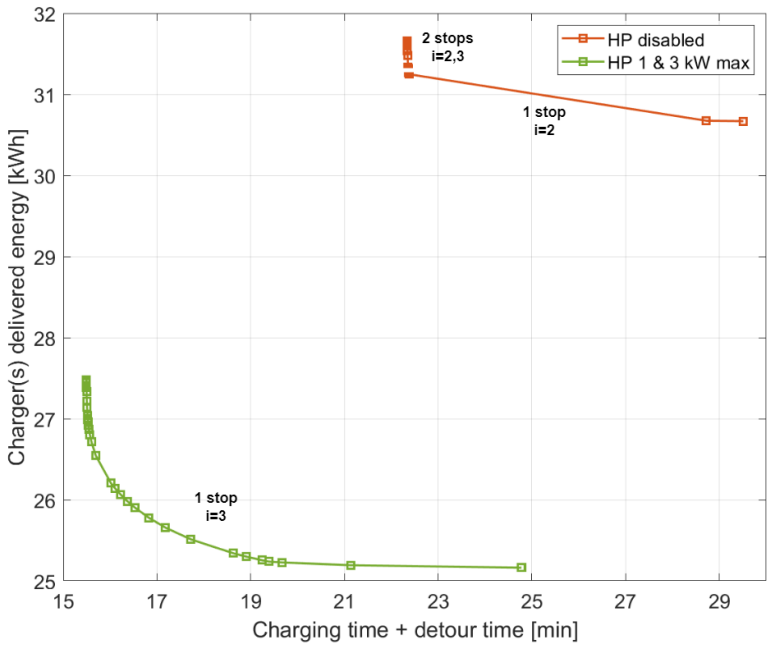

Figure 4.3: Ambient temperature of 0°C.

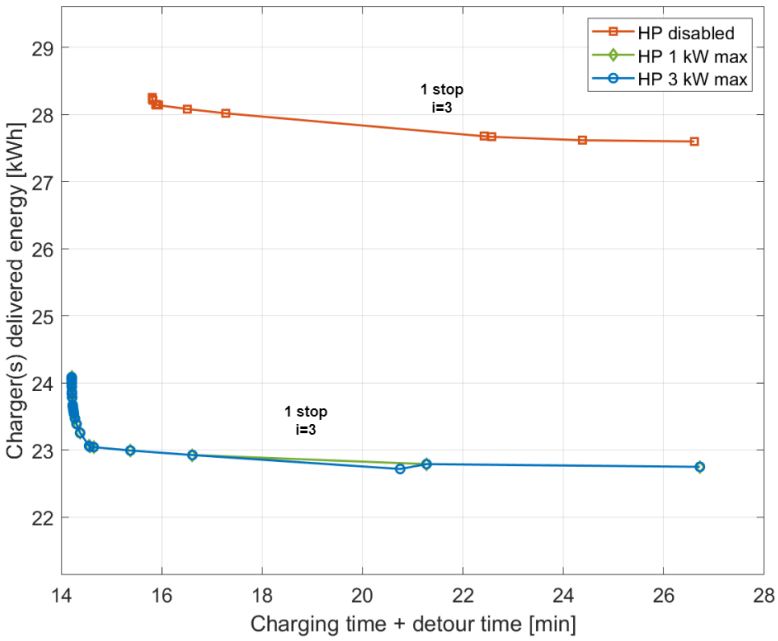

Figure 4.4: Ambient temperature of 10°C.

The following tables summarise the energy and time reductions at the different ambient temperatures.

	HP disabled	HP 1 kW max	HP 3 kW max
Energy at 28 min	38.40	34.13	32.69
Reduction	-	11.1%	14.9%
Time at time-opt. case	25.85	24.18	23.47
Reduction	-	6.5%	9.2%

Table 4.2: Energy and time comparisons at -10°C ambient temperature. Energy in kWh and time in minutes.

	HP disabled	HP 1 kW max	HP 3 kW max
Energy at 22.4 min	31.25	25.19	25.19
Reduction	-	19.4%	19.4%
Time at time-opt. case	22.34	15.50	15.50
Reduction	-	30.6%	30.6%

Table 4.3: Energy and time comparisons at 0°C ambient temperature. Energy in kWh and time in minutes.

	HP disabled	HP 1 kW max	HP 3 kW max
Energy at 16.5 min	28.08	22.92	22.92
Reduction	-	18.4%	18.4%
Time at time-opt. case	15.81	14.21	14.21
Reduction	-	10.1%	10.1%

Table 4.4: Energy and time comparisons at 10°C ambient temperature. Energy in kWh and time in minutes.

Comparing the relationship between charging and detour time and the energy delivered by the charger(s) at -10°C ambient temperature, the cases that have the HP activated have reduced energy use. The energy reduction at 28 min of combined charging and detour time is 11% for the 1 kW limited HP and 15% for the 3 kW limit. This reduction is due to the HP being used to move heat from the battery loop into the cabin compartment, reducing the need for the HVCH to be used for cabin heating.

When examining the time optimal solutions at -10°C for the different cases, the HP also allows for shorter combined charging and detour time, leading to a shorter total trip time. In terms of charging and detour time, the observed reduction is 6% and 9% for the 1 kW and 3 kW HP limits, respectively. This time difference is firstly the result of more efficient cabin heating during driving, increasing grid-to-wheel efficiency and thus reducing the amount of energy needed at a given charging stop. The second factor is detour time, which can be reduced in cases where it is infeasible to finish the trip with just one charging stop with the HP disabled, while it is possible with it enabled. That would lower the detour time directly by the number of stops avoided by using the HP.

At lower temperatures, limiting the HP to 1 kW rather than 3 kW has an effect on energy and time performance. This is due to a combination of high cabin heating demand and reduced COP at low battery temperatures, resulting in the need for more than 1 kW of HP compressor power to maintain the cabin climate, which means that the more limited case has to supplement cabin heating with the HVCH, while the other case is able to supplement less or not at all.

4.2.1 Energy Optimal Cases A-C

The following section examines cases A-C from Figure 4.2 in detail.

Case A (1 kW Heat Pump Limit)

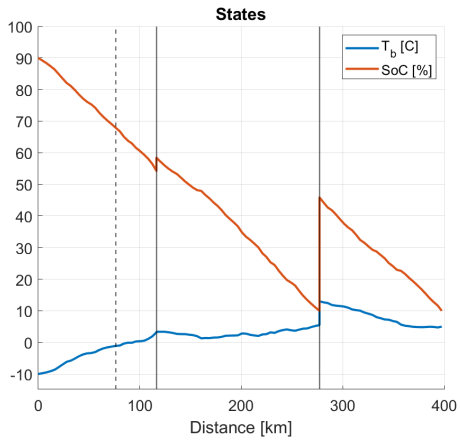

(a) States driving.

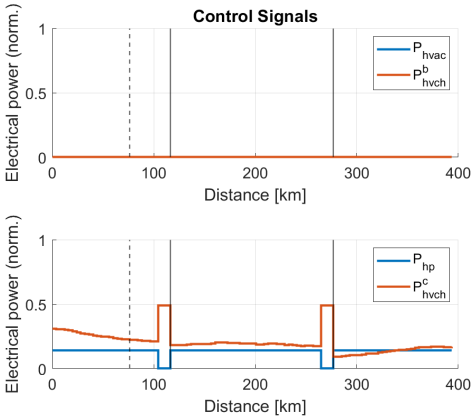

(b) Control signals driving.

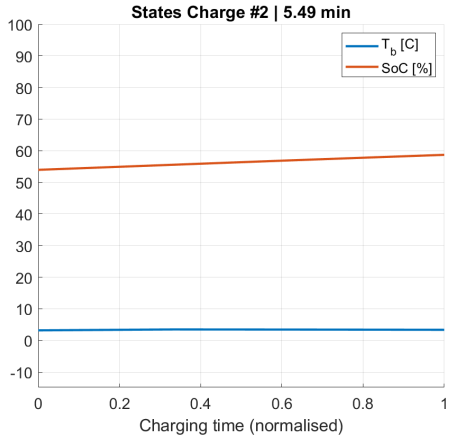

(c) States charging stop 1, 5.49 minutes.

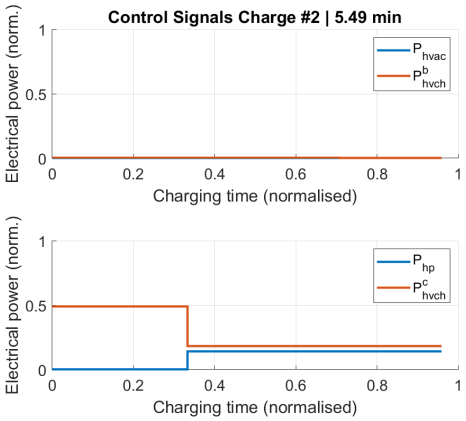

(d) Control signals charging stop 1.

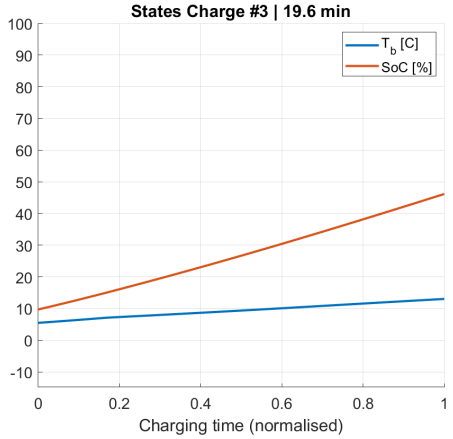

(e) States charging stop 2, 19.6 minutes.

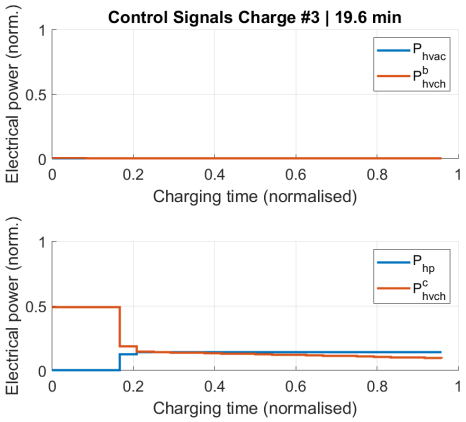

(f) Control signals charging stop 2.

Figure 4.5: Energy optimal case. Ambient temperature of -10°C and HP limited to 1 kW max.

Taking a closer look at the energy optimal case of the 1 kW HP limit at -10°C, the solution involves stopping twice. This indicates that the energy associated with the extra detour of stopping twice is less than the energy required to stay for longer at an early stop. Performing just one charging stop would in this case mean charging in the higher SoC region with reduced charging speed, leading to a longer charging time and more energy spent on maintaining cabin climate and supplying auxiliary loads.

The HVCH is not used for battery heating at all in this case in order to minimise unnecessary heat losses to the ambient environment. However, the HP is switched off right before charging and stays off during a portion of the charging stops, as seen in figures 4.5 (b), (d), and (f), meaning that some of the joule and ED losses are prioritised for battery heating. Doing so right before charging as well as during charging is reasonable, since that is when the higher battery temperature is useful and desirable to allow for faster-charging speed.

Case B (3 kW Heat Pump Limit)

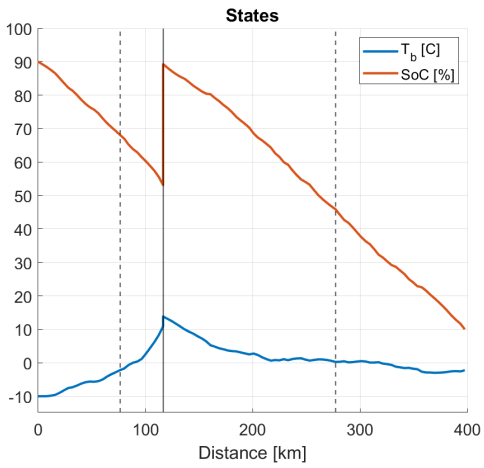

(a) States driving.

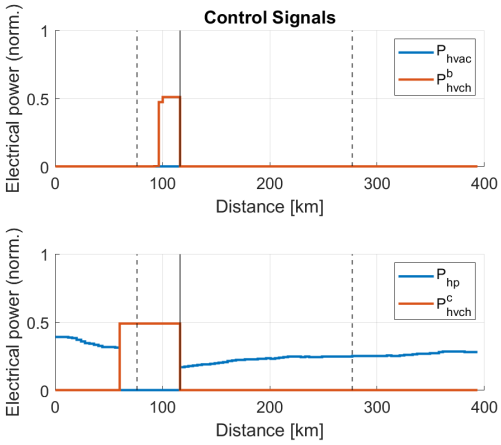

(b) Control signals driving.

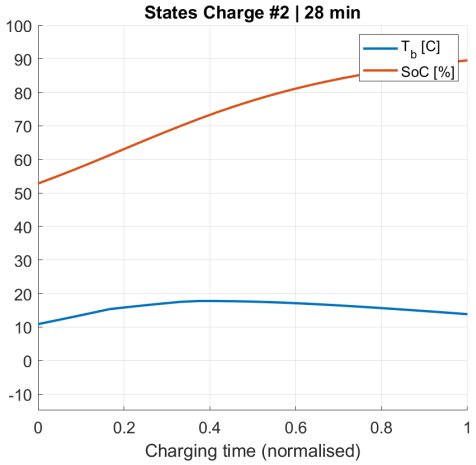

(c) States charging stop, 28 minutes.

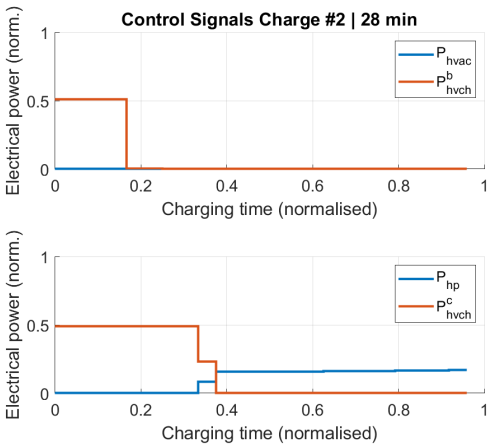

(d) Control signals charging stop.

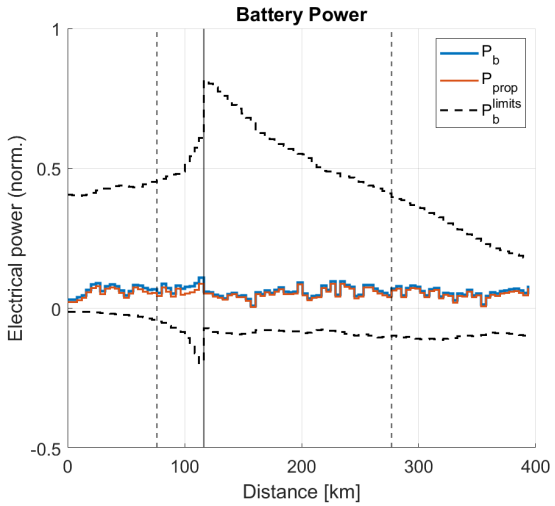

(e) Battery and propulsion power driving.

Figure 4.6: Energy optimal case. Ambient temperature of -10°C and HP limited to 3 kW max.

Changing the HP maximum power to 3 kW affects the solution significantly. Only one stop is performed, and the HVCH is used for battery heating before the charging stop and some time during the charging stop.

Since only the HP is used for cabin heating after the charging stop, the battery temperature is kept low, especially when nearing the destination, where the battery temperature is below 0°C. This combined with low SoC means that the battery has significantly limited discharge capabilities, as can be seen in Figure 4.6 (e).

Case C (Heat Pump Disabled)

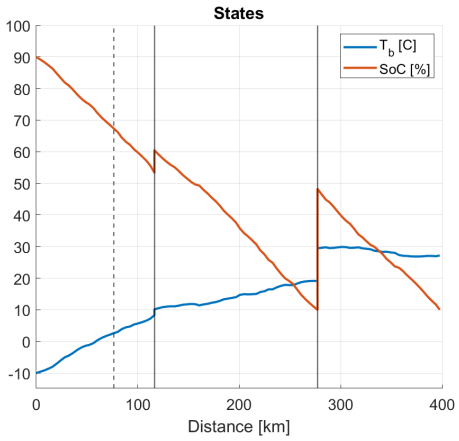

(a) States driving.

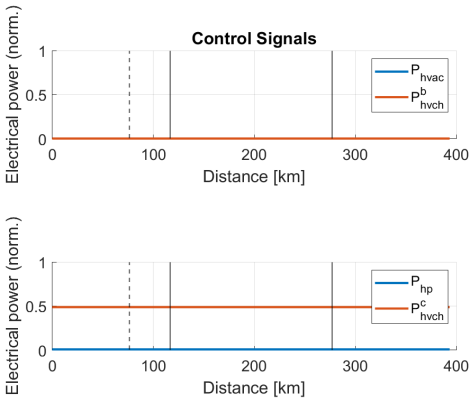

(b) Control signals driving.

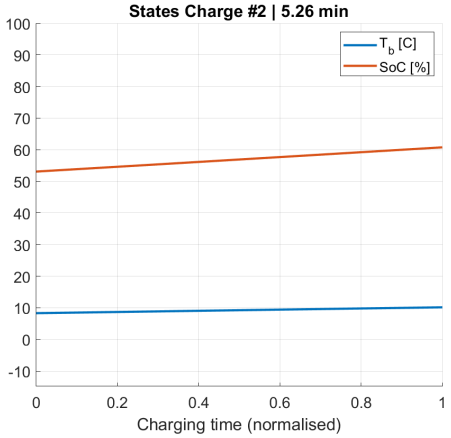

(c) States charging stop 1, 5.26 minutes.

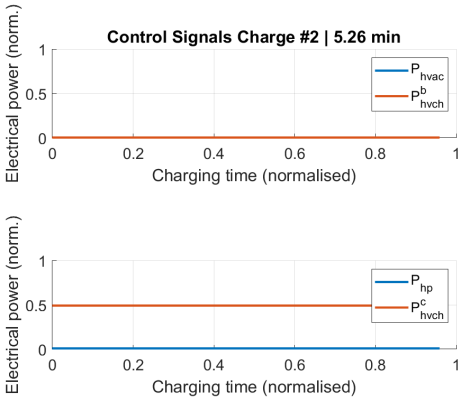

(d) Control signals charging stop 1.

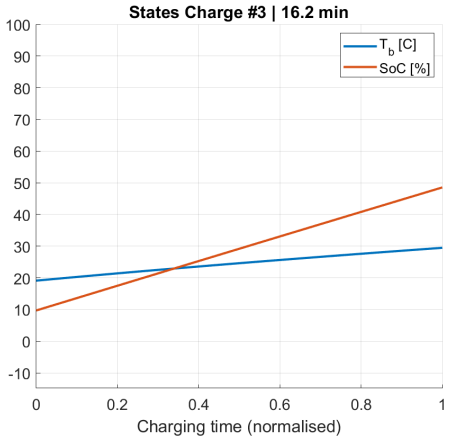

(e) States charging stop 2, 16.2 minutes.

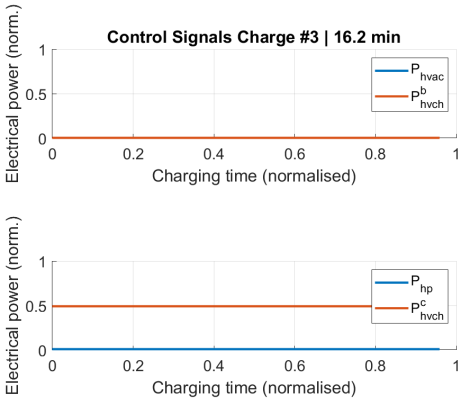

(f) Control signals charging stop 2.

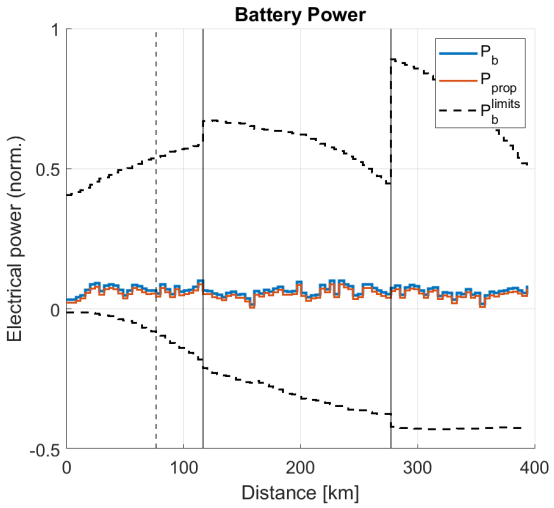

(g) Battery and propulsion power driving.

Figure 4.6: Energy optimal case. Ambient temperature of -10°C and HP disabled.

When the heat pump is disabled, two stops are performed before completing the trip. Even though no active battery heating using the HVCH is done, the battery temperature increases significantly over the course of the trip and levels out between 25 and 30°C at the end, as shown in Figure 4.6 (a). This is understandable since the only way for the battery to cool down without the HP is by active cooling using the HVAC, or by passive cooling to the ambient. Active cooling is not used in this case because the battery is kept below the maximum allowed temperature of 40°C with just passive cooling.

Compared to the 3 kW limited HP case, the maximum discharge power of the battery is kept at reasonable levels, as can be seen in Figure 4.6 (g), which is due to the overall higher battery temperatures.

4.2.2 Trade-off Case D

This section details case D from Figure 4.2, a trade-off between energy and time.

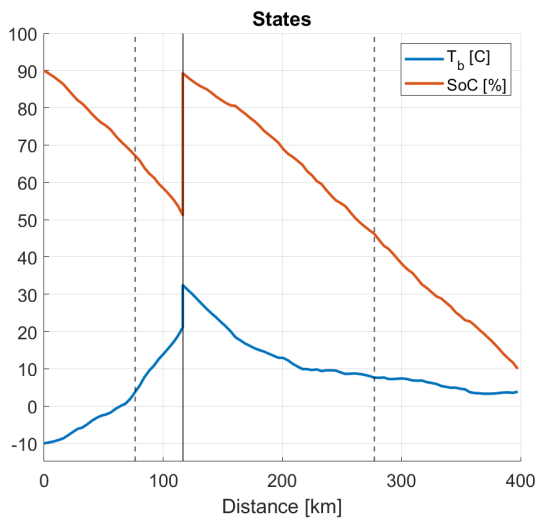

(a) States driving.

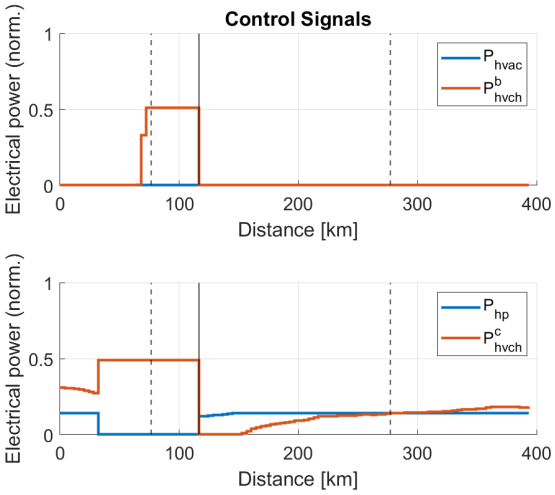

(b) Control signals driving.

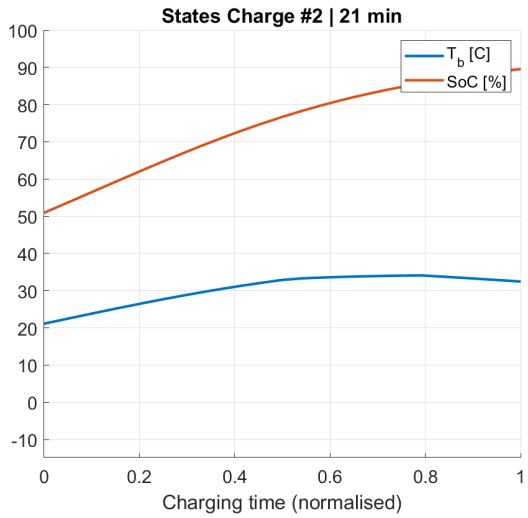

(c) States charging stop, 21 minutes.

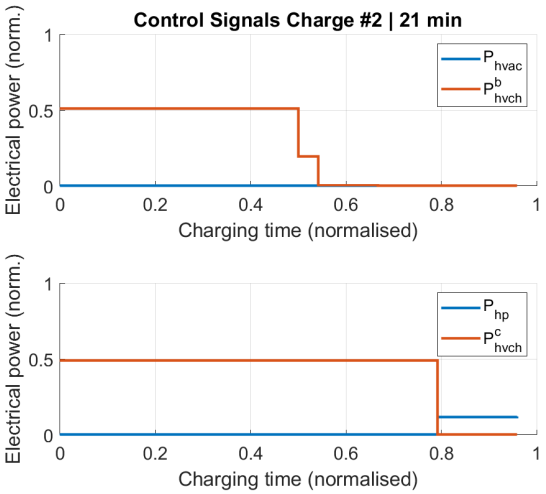

(d) Control signals charging stop.

Figure 4.7: Trade-off case. Ambient temperature of -10°C and HP limited to 1 kW max.

In the trade-off case, the solution differs both from the energy optimal and time optimal in the sense that only one charging stop is performed. Another major difference to the energy optimal case is the use of the HVCH for battery heating, both before and during the charging stop, to increase charging speed.

Even though charging at the early stage of the drive leads to longer charging time, in this case, the results indicate that the detour energy and/or detour time associated with stopping a second time is greater than the extra time and/or energy needed

for stopping early.

4.2.3 Time Optimal Case E

The final case E from Figure 4.2, which represents the time optimal solution, is examined in this section.

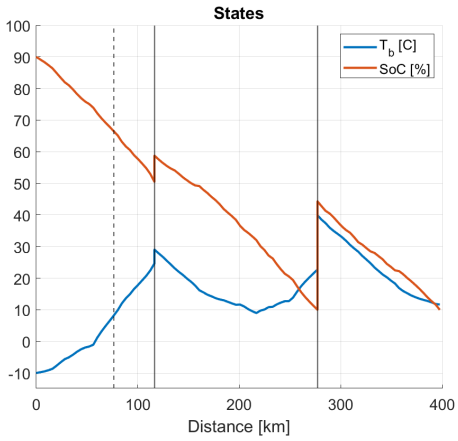

(a) States driving.

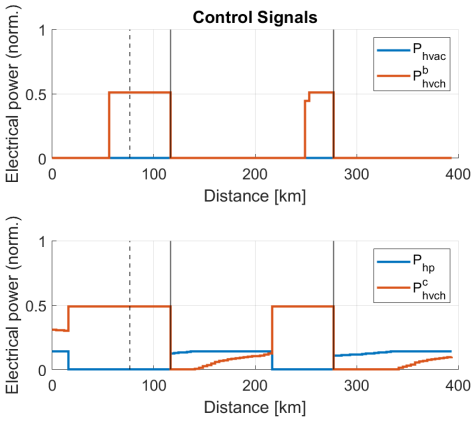

(b) Control signals driving.

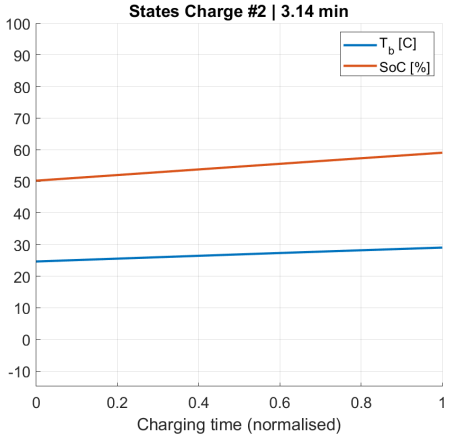

(c) States charging stop 1, 3.14 minutes.

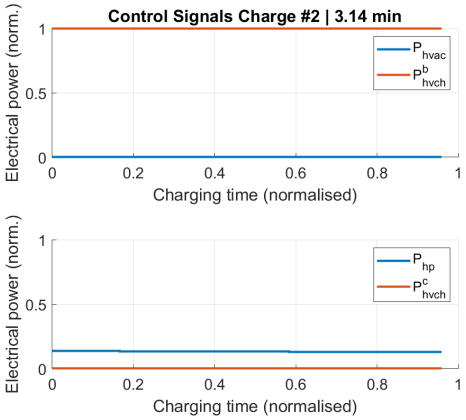

(d) Control signals charging stop 1.

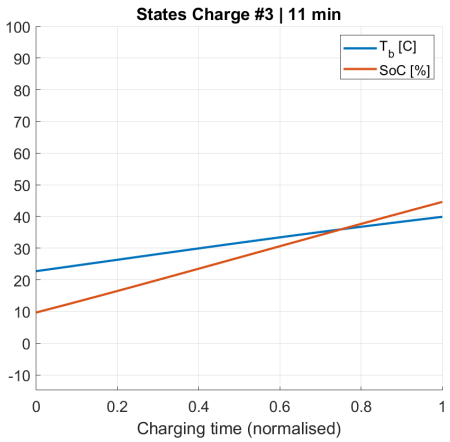

(e) States charging stop 2, 11 minutes.

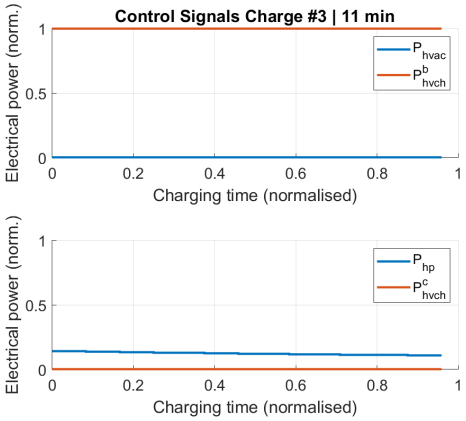

(f) Control signals charging stop 2.

Figure 4.8: Time optimal case. Ambient temperature of -10°C and HP limited to 1 kW max.

Just as in the energy optimal case, two charging stops are performed for the time optimal case. However, in contrast to the energy optimal case, pre-heating of the battery is done during driving to the point where the battery is close to the optimal temperature for fast charging speed when arriving at the charging stops.

During charging, the use of HVCH at full power for battery heating and HP for cabin heating at the same time is an effort to introduce the maximum amount of heat possible into the battery. The heat power provided for battery heating in this operating mode is greater than that when the HP was off and HVCH was split between the cabin and battery heating, since the HP compressor power itself is part of the heat delivered to the cabin. This means that the HP frees up the HVCH for maximum battery heating, while maintaining cabin heating demand. The gain in heat power for battery heating compared to only using the HVCH is equal to the HP compressor power.

4.3 Charged Energy vs. Ambient Temperature

The charged energy is compared over ambient temperature in this section. Time cost is fixed at 40 SEK/h for this comparison, which is the same time cost used for case D from Figure 4.2.

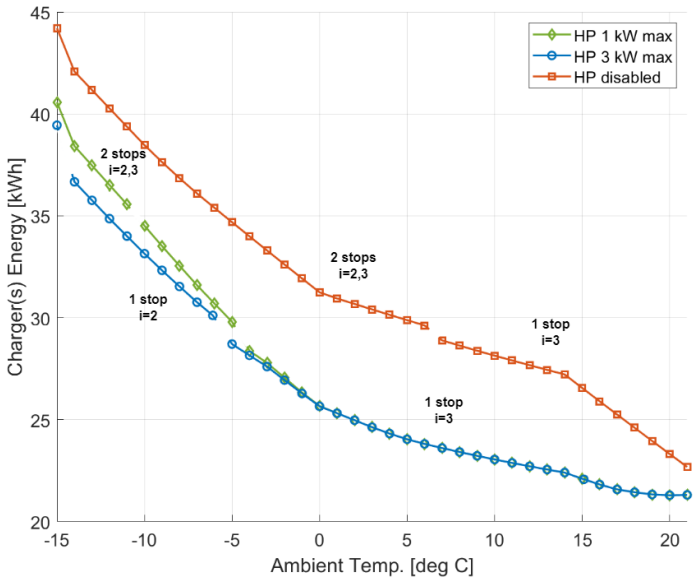

(a) Charged energy over ambient temperature.

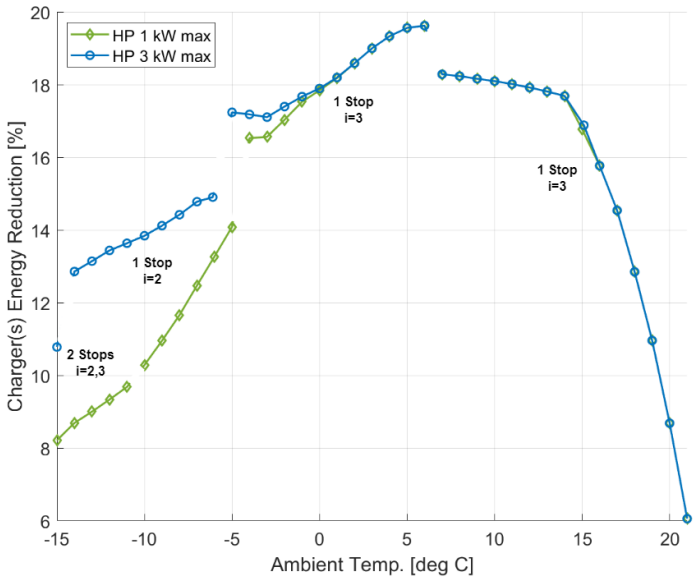

(b) Energy reduction compared to HP disabled over ambient temperature.

Figure 4.9: Comparison of energy delivered by charger(s) over ambient temperature.

At high ambient temperatures between 7 and 21°C, both the HP enabled and disabled cases are able to complete the trip with one late stop, meaning that they only stop at charge location #3, as seen in Figure 4.9 (a). However, as illustrated in Figure 4.9 (b), the HP enabled cases need between 6 and 18% less energy from the charger.

At 6 °C, the HP disabled case needs to stop twice, stopping at charge location #2 and #3. Because of the increased detour energy and time associated with stopping twice instead of once, a jump in energy reduction for the HP enabled cases is observed, up to between 19 and 20%.

As the temperature is reduced further, at 0 °C, a difference between the HP 1 kW limit and 3 kW limit case is noticeable. Once the temperature is reduced to -5 and -6°C, the 1 kW limit and 3 kW limit cases switch to performing one early stop at charge location #2, respectively. The reduction in energy drops when this switch occurs, not because the detour time or detour energy has changed, but because the time spent charging increases since the battery power is reduced when charging in the higher SoC region.

With the temperature reduced to -11°C, the 1 kW limit case starts to perform two stops, the same way as the HP disabled case. This switch happens for the 3 kW limit at -15°C.

5
Discussion and Conclusion

This final chapter discusses the results, covers suggestions for future work, and forms a conclusion to the thesis.

5.1 Thermal Management and Charging as Optimal Control Problem

When formulating and solving the thermal management and charging of BEVs as an optimal control problem, a couple of benefits over simpler methods, e.g. rule-based solutions, have become apparent. Firstly, the solution presented in this thesis is easy to adapt to changes in system features and parameters. This is illustrated by the results, where one implementation is used over a wide range of operating conditions, in terms of ambient temperatures and system features and constraints, e.g. availability of HP.

Secondly, combining the problem of thermal management with where and how to charge ensures that the solution considers how these two different problems can affect each other. Even though such a case was not investigated in this thesis, it is possible to imagine a case where the initial battery temperature for a long trip can affect where and how the charging should take place for optimal trip time and energy consumption.

5.2 Heat Pump for Improved Time and Energy Efficiency

Based on the results, the reduction both in terms of energy consumption as well as time spent charging and travelling to and from charging locations speaks in favour of including a heat pump for waste heat recovery in BEVs. The improvement varies significantly with ambient temperature, but as long as there is a heating demand for the cabin compartment, the case with a HP will perform better than the one without. This is the case even when the HP compressor power is limited, which indicates that even a small low-power HP can be useful in many cases, especially in milder climates.

However, the benefit of a HP may be limited in cases where there is limited waste heat available and there are constraints on the minimum allowed battery temperature, possibly due to limited discharge capability of the battery at low SoC and temperature.

5.3 Affects of Charge Point Optimisation

The inclusion of charge point optimisation leads to some interesting observations. For warmer ambient temperatures, the results in Figure 4.3 and 4.4 suggest that minimising the number of stops is best, regardless of priorities in terms of time or energy. However, for colder ambient temperature as in Figure 4.2 both the energy and time optimal solutions with HP disabled and with 1 kW HP limit, case A, C, and E, include two charging stops. It is only in the trade-off between these extremes, case D, that only one stop is performed for the 1 kW HP limit. Furthermore, for the 3 kW HP limit, only one stop is performed even at the coldest ambient temperatures. This may suggest that the increased consumption caused by higher demand for cabin heating, outweighs the cost in terms of energy and time that is associated with stopping frequently. By stopping more frequently in such a case, the time spent charging is reduced due to the charging taking place mostly in the lower SoC region, reducing the time spent keeping the cabin compartment warm.

With that said, there is some merit to the strategy of initially going as far as possible before stopping, then charging enough to make it to the next charging location. This is in fact the strategy used in e.g. the time and energy optimal cases for the 1 kW HP limit. However, as illustrated by the trade-off case D, there are cases where this strategy is not the optimal solution. In those cases, the optimal strategy is instead to minimise the number of stops, thus also minimising the energy and time associated with charging stop detours.

5.4 Conclusion

The problem of thermal management and charging of a BEV on a long trip can be formulated and solved as a non-linear, mixed integer optimal control problem. This formulation can be used to determine the trade-off between energy consumption and trip time, for different ambient temperatures and system features, such as a heat pump.

Using a heat pump for waste heat recovery in a BEV can reduce the energy consumption by up to 19.4%, or reduce the time needed for charging by up to 30.6% in cold environments.

By including charge point optimisation in the form of integer optimisation variables, the solution takes consequences related to where the charging stop(s) are made into consideration. The solution in terms of where to stop changes depending on variables

such as cabin heating demand, the availability of a HP, and the priority between time and energy.

5.5 Recommendations for Future Work

In this section the authors highlight a few areas that could be of interest for future work.

5.5.1 Inclusion of Speed optimisation

The current formulation can readily be extended to also include speed optimisation, where the longitudinal speed of the vehicle is included as an optimisation variable. By extending the problem in such a way, the solution would represent a more complete route optimisation that could be used to also control the cruise control of the vehicle, in order to further improve energy and/or time efficiency.

5.5.2 Extended Objective for More General Solutions

Currently, the objective function that is minimised is limiting the scope of the solution. In cases where it is possible to complete the trip without charging, the current formulation nets a cost of zero, since the costs are all related to charging stops. This is a problem, since if the cost is zero and there is no way to lower it further, the first solution that happens to complete the trip without charging would be considered optimal, even if that solution is sub-optimal in terms of energy extracted from the battery. This can be solved in a straight forward way by including a cost for energy extracted from the battery. Another option is to include a charging stop at the destination, and setting the final SoC constraint equal to the initial SoC.

Two other costs that can be included is a cost related to battery health and discharge power reserve. These costs then penalise high battery temperature and low maximum battery discharge power while driving, respectively.

5.5.3 Complexity Reduction for Enabling Online Optimisation

In order to enable this type of formulation to be solved online in a vehicle for model predictive control applications, significant reductions in computation time would be necessary. A first step can be to reduce the number of discretisation steps and investigate the trade-off between optimality and computation time in that respect.

One major factor that increases computation time significantly is the inclusion of integer optimisation variables. In the current formulation, integer, or more accurately, binary variables are used to decide if a charging stop is made or not. If the problem can be re-formulated such that these variables become real-valued, or if they can be removed altogether, the reduction in computation time would be significant.

Another option is to try to re-formulate the problem with the help of heuristics. For example, based on the results, if the HVCH is used for heating the battery before a charging event, the solution always involves running the HVCH at maximum power for some time right before the charging stop. This knowledge can be used to re-formulate the problem to control the average power or energy used for battery heating instead, which can allow for a significant reduction in discretisation steps, with a small or non-existent reduction in optimality.

Bibliography

[1] Iternio Planning AB. *A Better Route Planner*. URL: https://abetterrouteplanner.com/ (visited on 05/30/2022).

[2] Joel A E Andersson et al. "CasADi – A software framework for nonlinear optimization and optimal control". In: *Mathematical Programming Computation* 11.1 (2019), pp. 1–36. DOI: 10.1007/s12532-018-0139-4.

[3] Volvo Cars. *Volvo Cars to be fully electric by 2030*. URL: https://www.media.volvocars.com/global/en-gb/media/pressreleases/277409/volvo-cars-to-be-fully-electric-by-2030.

[4] Bicheng Chen et al. "A Comprehensive Thermal Model For System-Level Electric Drivetrain Simulation With Respect To Heat Exchange Between Components". In: *2020 19th IEEE Intersociety Conference on Thermal and Thermomechanical Phenomena in Electronic Systems (ITherm)*. 2020, pp. 558–567. DOI: 10.1109/ITherm45881.2020.9190448.

[5] Sourav Chowdhury et al. "Total Thermal Management of Battery Electric Vehicles (BEVs)". In: *SAE Technical Paper Series* 1 (May 2018). DOI: 10.4271/2018-37-0026. URL: https://www.osti.gov/biblio/1461757.

[6] Maximilian Cussigh and Thomas Hamacher. "Optimal Charging and Driving Strategies for Battery Electric Vehicles on Long Distance Trips: a Dynamic Programming Approach". In: *2019 IEEE Intelligent Vehicles Symposium (IV)*. 2019, pp. 2093–2098. DOI: 10.1109/IVS.2019.8813822.

[7] European Commission, Directorate-General for Climate Action. *amending Regulation (EU) 2019/631 as regards strengthening the CO2 emission performance standards for new passenger cars and new light commercial vehicles in line with the Union's increased climate ambition*. p. 14 https://eur-lex.europa.eu/legal-content/en/TXT/?uri=CELEX:52021PC0556. 2021.

[8] Toheed Ghandriz and Bengt J H Jacobson. *A Vehicle Longitudinal Dynamical Model for Propulsion System Tailoring*. 2020. URL: https://search.ebscohost.com/login.aspx?direct=true&db=ir01624a&AN=crp.7ede0621.e801.4227.b888.c2cbb7f06197&site=eds-live&scope=site&authtype=guest&custid=s3911979&groupid=main&profile=eds.

[9] Ahad Hamednia et al. "Computationally Efficient Algorithm for Eco-Driving Over Long Look-Ahead Horizons". In: *IEEE Transactions on Intelligent Transportation Systems* (2021), pp. 1–15. DOI: 10.1109/TITS.2021.3058418.

[10] Ahad Hamednia et al. *Optimal Thermal Management, Charging, and Eco-driving of Battery Electric Vehicles*. May 2022.

[11] Jorge Lopez-Sanz et al. “Nonlinear Model Predictive Control for Thermal Management in Plug-in Hybrid Electric Vehicles”. In: *IEEE Transactions on Vehicular Technology* 66.5 (2017), pp. 3632–3644. DOI: 10.1109/TVT.2016.2597242.

[12] Robin Lougee-Heimer. “The Common Optimization INterface for Operations Research”. In: *IBM Journal of Research and Development* 47(1) (Jan. 2003), pp. 57–66.

[13] Byrne Paul. “Research Summary and Literature Review on Modelling and Simulation of Heat Pumps for Simultaneous Heating and Cooling for Buildings.” In: *Energies* 15.3529 (2022), p. 3529. ISSN: 1996-1073. URL: https://search.ebscohost.com/login.aspx?direct=true&db=edsdoj&AN=edsdoj.7d465ae11a09427c99930d81beeb1d5d&site=eds-live&scope=site&authtype=guest&custid=s3911979&groupid=main&profile=eds.

[14] Tyler J. Shelly et al. “A Dynamic Simulation Framework for the Analysis of Battery Electric Vehicle Thermal Management Systems”. In: *2020 19th IEEE Intersociety Conference on Thermal and Thermomechanical Phenomena in Electronic Systems (ITherm)*. 2020, pp. 538–546. DOI: 10.1109/ITherm45881.2020.9190543.

[15] Tyler J. Shelly et al. “Comparative analysis of battery electric vehicle thermal management systems under long-range drive cycles”. In: *Applied Thermal Engineering* 198 (2021), p. 117506. ISSN: 1359-4311. DOI: https://doi.org/10.1016/j.applthermaleng.2021.117506. URL: https://www.sciencedirect.com/science/article/pii/S1359431121009388.

DEPARTMENT OF ELECTRICAL ENGINEERING
CHALMERS UNIVERSITY OF TECHNOLOGY
Gothenburg, Sweden
www.chalmers.se

CHALMERS
UNIVERSITY OF TECHNOLOGY